Artificial DNA in hydrology

Foppen, Jan Willem

DOI
10.1002/wat2.1681

Publication date
2023

Document Version
Final published version

Published in
Wiley Interdisciplinary Reviews: Water

Received: 13 December 2022 | Revised: 7 June 2023 | Accepted: 21 June 2023

DOI: 10.1002/wat2.1681

ADVANCED REVIEW

WIREs WATER WILEY

Artificial DNA in hydrology

Jan Willem Foppen

Water Resources Section, Department of Water Management, Faculty of Civil Engineering and Geosciences, Delft University of Technology, Delft, Netherlands

Correspondence
Jan Willem Foppen, Water Resources Section, Department of Water Management, Faculty of Civil Engineering and Geosciences, Delft University of Technology, Delft, Netherlands.
Email: j.w.a.foppen@tudelft.nl

Edited by: Wendy Jepson, Editor-in-Chief and Jan Seibert, Senior Editor

Abstract

The use of artificial DNA (artDNA) in hydrological applications is becoming increasingly popular, either in dissolved form (dissolved artDNA) or encapsulated and protected by a layer (encDNA). DNA can be detected even at low concentrations and offers the ability to create numerous uniquely identifiable DNA labels, making it ideal for a wide range of multi-tracer applications. A literature review revealed that in streams, the breakthrough curve of artDNA is visually similar to that of a conservative tracer in terms of time to rise, time to peak, and dispersion coefficient. In saturated porous or fractured media, the time of first arrivals and time to peak of artDNA are usually earlier than that of a conservative tracer, indicating size exclusion of both dissolved artDNA and encDNA. Transport in subsurface media can be described by one-site or two-site kinetic attachment. The recovery of artDNA in environmental systems is always less than 100% due to adsorption and decay. Although the processes responsible for both are known, yet they cannot be quantified or predicted in mass balance approaches. Despite these limitations, artDNA can be used in various hydrological applications in environmental studies and engineering. Finally, attention should focus on the use of rapid detection of DNA tracers in the field, on upscaling of DNA production, and on increasing the efficiency of the DNA encapsulation process.

This article is categorized under:
Science of Water > Hydrological Processes
Science of Water > Water Quality
Science of Water > Methods

KEYWORDS
colloids, DNA, eDNA, mass balance, tracer

1 | INTRODUCTION

Understanding the pathways of water flow and quantifying them is crucial for understanding mass migration in water systems, changes in water quality, and developing a deeper understanding of hydrology. Tracers play a pivotal role in achieving this. Tracers are "substances which can be detected in water at very low concentrations and allow following,

or tracing, the flow of water" (Leibundgut et al. (2009). Tracers can be environmental (tracers which are part of the hydrological system; also known as "passive" tracers) or artificial (brought into the hydrological system intentionally for tracer study, also known as "active" tracers). In order to examine ecohydrological and biogeochemical functioning beyond the scope of single proxies, multi-tracer techniques have been developed (Abbott et al., 2016; Ettayfi et al., 2012; González-Pinzõn et al., 2013; Kirchner, 2016a, 2016b; McDonnell & Beven, 2014; Oldham et al., 2013; Payn et al., 2008; Pinay et al., 2002; Urresti-Estala et al., 2015). Examples of artificial tracers include dissolved salts (sodium, potassium, lithium, chloride, bromide), organic solutes and fluorescence dyes (e.g., uranine or fluorescein, rhodamine), stable isotopes (e.g., deuterium) or particulates (e.g., yeast, spores, bacteria, and bacteriophages, clay, synthetic microparticles, and DNA; Abbott et al., 2016; Auckenthaler et al., 2002; Flynn & Sinreich, 2010; Goeppert & Goldscheider, 2019; Leibundgut et al., 2009; Richter et al., 2022; Schiperski et al., 2016). Of those, the artificial ones that have no or very limited interaction with the environment are called conservative. Both conservative and nonconservative (reactive) tracers are widely used in hydrological research. Evidently, it is more difficult to interpret nonconservative tracers, for example if tracer mass in water is lost (depleted) or enriched due to dissolution during its transport, as, in such case, reaction processes have to be taken into consideration in order to interpret the tracer experiment. Water travels in the environment, for example from precipitation in a catchment to the stream, via numerous flow paths and a broad spectrum of travel times, whereas the few tracers that exist give only limited insight in hydrological process dynamics. Also, the amount of water involved can dilute "away" the tracer, so the detection limit becomes an important constraint. Advancements in hydrological science demand new tracers, that can be detected at low concentrations, exhibit identical or nearly identical behavior, and offer an infinite number of uniquely identifiable tracers can be made. In theory, DNA fulfills most of these criteria, and an overview of the advantages of the use of DNA as a tracer system in hydrological applications has been given by Liao et al. (2018; their tab. 1).

Over the past two decades, a number of workers have used artificial DNA, or artDNA, in various forms and in various types of groundwater and surface water environments with varying degrees of success. The term artificial DNA is elaborated upon in the next section. This review primarily focuses on the injection of artDNA in surface water, groundwater, and in laboratory set-ups with the objective to understand artDNA transport behavior and demonstrate its potential and limitations in environmental applications. While Zhang and Huang (2022) recently reviewed the use of DNA based tracers for characterizing subsurface hydrogeological systems, this review concentrates on quantifying the mass balance of injected artDNA mass balance and elucidating the context-specific and environment-dependent mass balance terms of artificial DNA in both surface water and groundwater environments. This review begins by presenting and discussing the nomenclature related to DNA, followed by an evaluation of mass balance recoveries from injection experiments in Section 3. Section 4 delves into the explanation and detailed analysis of mass balance components. Sections 5, 6, and 7 cover challenges, research directions, and concluding remarks, respectively.

2 | DISSOLVED artDNA AND encDNA

According to Wikipedia, DNA (Figure 1) is "a polymer composed of two polynucleotide chains that coil around each other to form a double helix carrying genetic instructions for the development, functioning, growth and reproduction of all known organisms and many viruses. DNA and ribonucleic acid (RNA) are nucleic acids. Alongside proteins, lipids and complex carbohydrates (polysaccharides), nucleic acids are one of the four major types of macromolecules that are essential for all known forms of life."

In hydrological applications, use is made of artificially prepared single stranded or double stranded DNA molecules with a limited number of nucleotides (nt), ranging from 50 to 500 nt. Usually, these molecules are prepared in a DNA production laboratory, hence the name artificial DNA, or in short artDNA. When in water, artDNA is essentially dissolved artDNA (see Box 1). As was pointed out by Liao et al. (2018), the avoidance of background from ambient DNA of organisms is a crucial factor in the nt sequence of the constructed DNA molecule. DNA tracer sequences should be separated from environmental genetic background DNA. The constructed DNA must be checked to ensure specificity using the free-to-use software program BLAST (http://www.ncbi.nlm.nih.gov/). More DNA design considerations are given in Zhang and Huang (2022), Foppen et al. (2011), Foppen et al. (2013) and Liao et al. (2018).The length of ssDNA is ~0.7 nm per base (Zhang et al., 2021), while, due to the presence of helical folding the length of dsDNA is ~0.34 nm per base pair (Yan & Marko, 2004). Dissolved DNA is essentially a colloidal biopolymer, which can be used as a food source, can take part in chemical reactions, and is subject to various enzymatic influences.

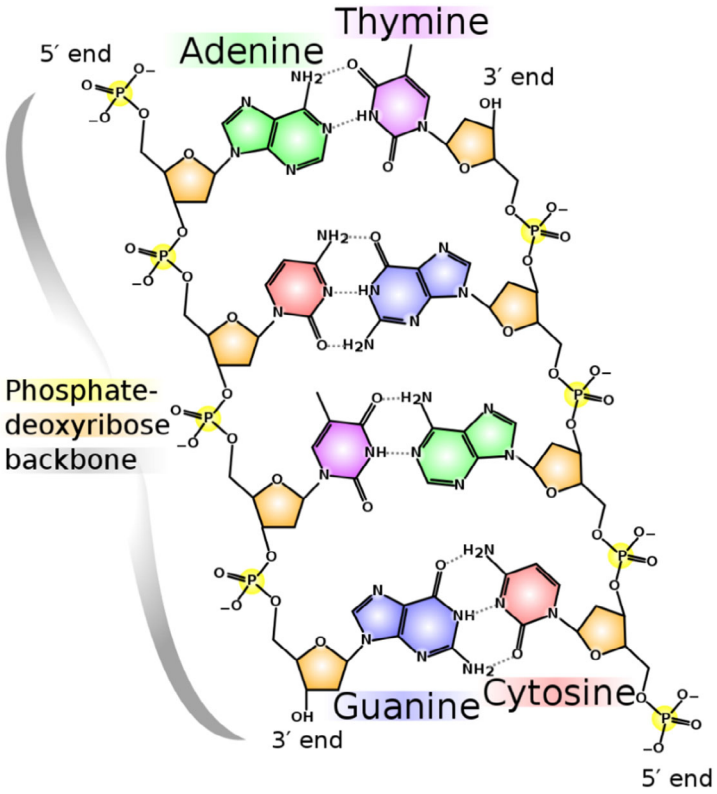

FIGURE 1 A piece of double stranded DNA with on the left-hand side a phosphate deoxyribose backbone including—from top to bottom—bases A-C-T-G and on the right-hand side the complementary strand T-G-A-C with phosphate-deoxyribose backbone. *Source*: Madeleine Price Ball, Wikimedia Commons.

BOX 1 Environmental DNA and dissolved DNA

Environmental DNA or eDNA is defined as "a total pool of DNA isolated from environmental samples" (Pawlowski et al., 2020; Rodriguez-Ezpeleta et al., 2021; Taberlet et al., 2012). According to Pawlowski et al. (2020) "this general concept assumes that eDNA is defined primarily by its origin and not by its taxonomic composition or its specific structural state (intra- or extracellular)."

A part of eDNA can become extracellular or dissolved in water upon lysis of cells or cell parts in which the DNA was contained (Mauvisseau et al., 2022), hence the term dissolved DNA. Also, freshwater bacteria can simply produce dissolved DNA: in one investigation, 25 out of 110 bacterial isolates produced significant quantities of dissolved DNA (Morales-Garcia et al., 2021). For instance, in the stationary phase of Pseudomonas sp. FW1, dissolved DNA accumulated and connected cells into a filamentous mesh. Though less studied, also in groundwater environments dissolved DNA was found (Niemiller et al., 2017; van den Berg-Stein et al., 2022). Dissolved DNA can be adsorbed to particulate matter (e.g., geo-colloids, natural organic matter), and then it is called adsorbed DNA (Mauvisseau et al., 2022).

To prevent DNA decay, artDNA can be encapsulated, resulting in encapsulated DNA, or encDNA. In contrast to dissolved DNA, encDNA is a colloidal particle with a certain size (usually less than 1 μm) and surface charge. EncDNA is not considered to be a good food source, although Mikutis et al. (2018) reported encDNA loss due to microbial activity inside sample bottles. Also, encDNA is not thought to take part in chemical reactions, or subject to enzymatic influences. Compared to dissolved artDNA, for encDNA additional work flow in the laboratory is required to encapsulate the DNA and to release DNA for quantification (Zhang & Huang, 2022).There are six types of DNA encapsulates for hydrological applications used in literature (Figure 2):

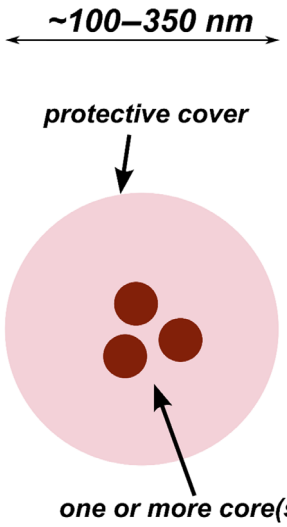

FIGURE 2 Summary design of encDNA. The particle is composed of one or more cores of superparamagnetic iron, silica or DNA-chitosan. The iron and silica core(s) are then surrounded by DNA. Core(s) plus DNA are finally wrapped in a protective layer of PLA, silica, or alginate. Size of most particles in use is 100–350 nm; for some designs (PLA and silica) size can be tuned to smaller (50 nm) or larger (1000 nm). The Garnett particle is smaller (35 nm), while the Liao particle is much larger (>200,000 nm).

1. The particle produced by Garnett et al. (2009) was around 35 nm in size and was made of DNA that had been circumferentially wrapped in a condensed form. The particle was stabilized using a self-assembling system that included poly-amidoamine (PAA), a cationic homopolymer, and a PEG [poly(ethylene) glycol]-PAA-PEG copolymer. The resulting particle resembled a polymer "cage" with DNA inside; decay or degradation of the particle for hydrological applications was not determined.
2. The particle produced by Sharma et al. (2012) and subsequently reproduced by Dahlke et al. (2015) had an approximate size of 480 nm, was composed of a core of iron oxide nanoparticles plus DNA, and encapsulated by polylactic acid (PLA) For particles in the range of 60 to 930 nm, for a number of environmentally relevant conditions, McNew et al. (2018) found that the DNA label concentration remained relatively constant on the order of 10 days, and then, a steady decline was observed. After some 220 days, DNA concentrations in all batch experiments were only 1 log unit above detection limit.
3. The particle used by Mikutis et al. (2018) was reproduced from Paunescu et al. (2013) and had a silica core, surrounded by a layer of DNA, and protected by an outer cover of—again—silica. The size of the particle could be controlled, and ranged from 150 to 1000 nm. However, more commonly, the particle size was in the range of 140–270 nm (Kianfar et al., 2022; Kittilä et al., 2019; Kong et al., 2018; Tang et al., 2021). Using this silica protection, DNA damage by radical oxygen treatment was limited (Paunescu et al., 2013). In addition, in an accelerated aging test, a similar silica cover protected the particles to an equivalent of 2 year at room temperature without substantial loss (Puddu et al., 2014).
4. The particle produced by Pang et al. (2020) was composed of dsDNA-chitosan with an alginate cover. The mean size of the microparticles was 312 (±132) nm. Over the course of 8 days, the particles remained stable in distilled water with only a 0.1 log decline in concentrations. Furthermore, after being exposed to light/dark cycles at 20°C for 4 days, the DNA content in stream water did not decrease, but some DNA from the particles had been dispersed into the solution again.
5. The particle produced by Liao et al. (2020) had a core of superparamagnetic iron and plasmid DNA (pDNA) encapsulated by PLGA. The size of the particles was in the range of 246 μm, which is about 1000–10,000 times larger than the particles mentioned above. Unlike the others, the Liao particle floated. The main advantage of using plasmid-DNA was the ability to cost-effectively produce large quantities of pDNA. The particles were well protected against high temperature, intensive UV radiation (50 J/cm^2), DNAse, and saline treatment. It should be noted, however, that Liao and workers mostly evaluated the effect of treatment on protection of DNA using classical end-point PCR, which made a quantitative assessment of the various treatments difficult.

6. Recently, Tang et al. (2023) used silica encapsulated DNA containing a few ~20 nm superparamagnetic iron cores, as originally designed by Puddu et al. (2014) and later optimized by Sharma et al. (2021). These superparamagnetic iron cores were surrounded by a layer of DNA, and protected by an outer cover of silica. The size of the particle was ~200 nm. Advantage of these particles is the possibility to magnetically retrieve or harvest them from complex water matrices, which may confound the qPCR signal (e.g., inhibition).

3 | MASS BALANCE RECOVERIES OF ARTIFICIAL DNA EXPERIMENTS

3.1 | Dissolved artDNA

In the case of injecting dissolved artDNA in streams, the determined (relative) mass recoveries ranged between less than 1% to at most 57% for stretch lengths between 28 and 1192 m (Table 1). In those cases, mass recoveries of conservative tracer were usually in the order of 90%–100%. This indicated that dissolved artDNA did not behave in the same way as a conservative tracer. Relative dissolved artDNA mass recoveries (RB; see Tables 1 and 2) were defined as the ratio of dissolved artDNA mass recovery to the mass recovery of a conservative tracer. When comparing shapes of dissolved artDNA breakthrough curves in terms of time to rise, time to peak, and dispersion coefficient with the breakthrough curve of a conservative tracer, then from visual inspection, in most cases these values were similar. However, McCluskey et al. (2021) reported an earlier breakthrough in their surface water injection experiment, which they attributed to the dispersion of artDNA into fewer flow paths compared to dye tracers, suggesting a preferential travel of artDNA through the stream.

For dissolved artDNA injected into saturated sand or glass bead column experiments, (relative) mass recoveries ranged from 0.009% to 74%. Aquilanti et al. (2013) were the only ones to report no removal, resulting in artDNA mass recoveries of ~100%. In the case of glass bead columns, Zhang et al. (2021) observed DNA length dependent (90–200 bp) mass recovery, whereby DNA recovery increased with increasing DNA length (80%–114% mass recovery). Breakthrough of dissolved artDNA was sometimes earlier than that of a conservative tracer (Aquilanti et al., 2013; McCluskey et al., 2021; Pang et al., 2017; Pang et al., 2020; Ptak et al., 2004; Zhang et al., 2021), but breakthrough could also be significantly retarded (Zhang et al., 2021; their sand column tests). Zhang et al. also noted that the length of the artDNA did not significantly affect peak arrival or dispersion behavior.

For dissolved artDNA injected into aquifers, only Pang et al. (2017, 2020) determined relative mass recoveries, which ranged from less than 0.0001% to 76%, dependent on aquifer type (in their case: fine coastal sand versus alluvial gravel). From this, Pang et al. (2020) concluded that artDNA should not be utilized in these fine sands, which also included pumice fragments with a high affinity for negatively charged DNA. The transport distance of artDNA ranged from few meter (Sabir et al., 1999) to ~2 km (Aquilanti et al., 2013). Finally, in a transient variably saturated sloping lysimeter filled with freshly crushed basaltic tephra, the mass recovery of dissolved artDNA was 1.05% (Wang et al., 2022).

3.2 | EncDNA

The following comparison essentially applies to the size of the particle and the differences in cover used to protect artDNA, and is not applicable to artDNA itself (Table 2). In surface water injection experiments, (relative) mass recoveries of the various encDNA particle types ranged from 6% to 111%, which was generally higher than the (relative) mass recoveries of dissolved artDNA. Both Dahlke et al. (2015) and Pang et al. (2020), who applied both dissolved and encDNA under the same conditions, reported higher (relative) mass recoveries for encapsulated artDNA than for dissolved artDNA. However, like dissolved artDNA, also protected or encapsulated DNA did not behave in a conservative way.

In column experiments, Mikutis et al. (2018) and Pang et al. (2020) reported mass recoveries ranging from 0.01% to 85.9%, depending on cover-type (silica or alginate). Chakraborty et al. (2022) reported mass recoveries in their 15 cm columns ranging from 10% to 83% as a function of silica covered artDNA particle injection concentration. Kianfar et al. (2022) did not specifically report mass recoveries; however, based on maximum relative concentrations, mass recoveries were in the range of ~90% for demineralized water experiments, from ~2% to 90% in case of NaCl type water used, and

TABLE 1 Overview of dissolved artDNA tests carried out.

	Set-up	DNA used	Size	Detection	Dissolved artDNA mass recovered	Decay	Aggregation	Stretch length	Reference
Surface water injection	Two brooks in the NL/Belgium	ssDNA	80 nt	qPCR	n.d.	n.d.	n.d.	112–1192 m	Foppen et al., 2011
	Various small reaches with low discharge in Benelux	ssDNA	80 nt	qPCR	3%–53%; NaCl: 66%–106%	Decay nihil; initial losses of 40%–97%	Attachment rate coefficient = 0–0.2/h	100–650 m	Foppen et al., 2013
	Small glacier in Sweden	ssDNA	90–99 nt	qPCR	1%–57%; dye: 99%	Nihil (assumed)	n.d.	~500–1000 m	Dahlke et al., 2015
	Coldstream in New Zealand	dsDNA	352 bp	qPCR	RB: from ~1% at 100 m to ~0.05% at 600 m to ~0.01% at 1000 m	River: 0.039–0.118 h^{-1}; river with 5% dairy effluent: 0.241–0.347 h^{-1}	n.d.	20–1000 m	Pang et al., 2020
	Southern reach of Helotes Creek, Texas	dsDNA	300 bp	ddPCR	n.d.	One-phase decay pattern at different temperatures (k = 0.125–0.071 h^{-1})	n.d.	28–42 m	McCluskey et al., 2021

	Column	DNA used	Size	Detection	Dissolved artDNA mass recovered	Decay	Sorption or attachment	Column length	
Column experiment	Undisturbed core Lauswiesen test site	ssDNA	90 nt	qPCR	n.d.	n.d.	n.d.	50 cm	Ptak et al., 2004
	Repacked aquifer material	ssDNA	72 nt	qPCR	n.d.	n.d.	Nihil	20 and 45 cm	Aquilanti et al., 2013
	Repacked aquifer material (alluvial gravel)	dsDNA	302 bp	qPCR	RB: 45%–50%	n.d.	n.d.	2 m	Pang et al., 2017
	Intact topsoil and 0.4 m sandy gravel vadose zone material	dsDNA	302 bp	qPCR	RB: 0.1%–74% with autoclaved effluent RB: 0.009%–3% with non-autoclaved effluent	n.d.	n.d.	0.7 m (lysimeter)	Pang et al., 2017
	Same as above	dsDNA	352 bp	qPCR	RB ≤ ~1%	n.d.	n.d.	0.7 m (lysimeter)	Pang et al., 2020
	Repacked dry natural play sand and crushed limestone	dsDNA	300 bp	ddPCR	RB: 26%	Nihil (assumed)	n.d.	25.4 cm	McCluskey et al., 2021
	Glass beads; Ottawa sand	dsDNA	90–200 bp	qPCR	RB in glass beads: 80%–114% RB in sand: 16%–21%	n.d.	(Sorption coeff part coeff) Glass: 3.8E-9-5.4E-12 ms^{-1} Sand: 1.5E-8- 2.0E-8 ms^{-1}	50 cm	Zhang et al., 2021

TABLE 1 (Continued)

	Column	DNA used	Size	Detection	Dissolved artDNA mass recovered	Decay	Sorption or attachment	Column length	
	Freshly crushed basaltic tephra (transiently saturated)	ssDNA	87 nt	qPCR	1.05%; Deuterium: 97.8%	7.3E-6 min^{-1} (from trial and error during modeling)	ka1 = 1.58E-3; kd1 = 1.24E-3; ka2 = 1.96E-3; kd2 = 5.72E-6	Tilted tank: 200 × 50 × 100 cm (L × W × D); bed slope = 10°	Wang et al., 2022
	Aquifer	**DNA used**	**Size**	**Detection**	**Dissolved artDNA mass recovered**	**Decay**	**Sorption or attachment**	**Distance traveled**	
Injection into aquifer	Glaciofluvial sand aquifer	ssDNA	72 nt	PCR	n.d.	n.d.	n.d.	~8 m	Sabir et al., 1999
	Alluvial aquifer (Lauswiesen site)	ssDNA	90 nt	qPCR	n.d.	n.d.	n.d.	?	Ptak et al., 2004
	Karstic sinkhole and springs	ssDNA	72 nt	qPCR	n.d.	n.d.	n.d.	~2 km	Aquilanti et al., 2013
	Karstic sinkhole and springs	ssDNA	72 nt	qPCR	n.d.	n.d.	n.d.	1.8–2.0 km	Aquilanti et al., 2016
	Alluvial aquifer	dsDNA	302 bp	qPCR	RB: 47%–76%	n.d.	n.d.	12–37 m	Pang et al., 2017
	Alluvial aquifer	ssDNA	72 nt	qPCR	n.d.	n.d.	n.d.	Single well dilution test	Tazioli et al., 2019
	Alluvial gravel aquifer fine coastal sand aquifer	dsDNA	352 bp	qPCR	RB (at 21 m site; alluvial aquifer): 0.01–0.03% RB(fine coastal sand aquifer): ~0.0001%	n.d.	n.d.	37–62 m	Pang et al., 2020

Note: Mass recovery: artDNA mass recovery compared to mass injected; relative mass recovery (RB): artDNA mass recovery compared to mass recovery of a conservative tracer.
Abbreviations: ds, double stranded; n.d., not determined; RB, relative mass recovery; ss, single stranded.

TABLE 2 Overview of encDNA tests carried out.

	Set-up	Protection	DNA tracer used	Size	Detection	encDNA mass recovered	Aggregation	Stretch length	Sticking efficiency	Reference
Surface water injection	River Fruin	Polymer cage	60–80 nt (ss?DNA)	20–200 nm diameter	qPCR	n.d.	n.d.	6.1 km	n.d.	Garnett et al., 2009
	Small stream reach	PLA	ss?DNA, 100 nucleotides	DLS: 480 ± 59 nm	qPCR	n.d.	n.d.	6–61 m	n.d.	Sharma et al., 2012
	Injection into a small glacier	PLA	82–102 nt	Not mentioned	qPCR	6%–66%; dye: 99%	n.d.	~500–1000 m	n.d.	Dahlke et al., 2015
	Coldstream	Alginate	dsDNA, 352 bp	312 ± 132 nm	qPCR	RB: 10%–100%	n.d.	20–1000 m	n.d.	Pang et al., 2020
	Injection in an artificial channel	PLA	pDNA, few 1000 bp	246 ± 56 μm	Mostly PCR	n.d.	n.d.	5 m	n.d.	Liao et al., 2020
	Injection in surface water channel (laboratory)	Silica	dsDNA, 65 bp, same as Mikutis et al., 2018	DLS: 200–300 nm	qPCR	80%–111%; NaCl: ~100%	Possibly shear-induced	0.2 m	n.d.	Tang et al., 2021

	Column	Protection	DNA tracer used	Size	Detection	encDNA mass recovered	Sorption or attachment	Column length	Sticking efficiency	Reference
Column experiment	Aquifer of grade 12/20	PLA	ss?DNA, 100 nt	DLS: 480 ± 59 nm	qPCR	n.d.	n.d.	24.5 cm	n.d.	Sharma et al., 2012
	Fine beach sand (mean grain size 0.19 mm)	None	dsDNA (312 bp) on protein-coated silica nanoparticles	Si core = 70 nm	qPCR	RB = 0.35	Determined, used for sticking efficiency	30 cm	0.001	Pang et al., 2014
	Sand	Silica	dsDNA, 113 bp	200 nm	SEM observation of effluent	n.d.	n.d.	2 inch	n.d.	Zhang et al., 2015; 2016
	Sediment mixture, wet-sieved to 0.20–0.63 mm sand	Silica	SiDNASi, dsDNA, 76–108 bp	150, 159, 410, 848 nm	qPCR	85.9% for W-1 (159 nm), 56.3% for W-2 and 39.3% for W-3 (848 nm); 67.4% for uranine	Deposition rate increased roughly linearly from 0.008 min^{-1} for 159 nm particles to 0.034 min^{-1} for 848 nm ones.	29.6 cm	n.d.	Mikutis et al., 2018
	0.3 m intact topsoil and 0.4 m sandy gravel vadose zone material	Alginate	dsDNA, 352 bp	312 ± 132 nm	qPCR	RB: ~0.01% for K2 enc (lysimeter experiment 3)	n.d.	0.7 m	n.d.	Pang et al., 2020

TABLE 2 (Continued)

	Column	Protection	DNA tracer used	Size	Detection	encDNA mass recovered	Sorption or attachment	Column length	Sticking efficiency	Reference
	Coarse sand: 1000–1400 μm; fine sand: 500–630 μm	Silica	dsDNA, 80 bp	270 nm	qPCR	DM: ~90% NaCl: ~2%–90% CaCl2: ~4%–50% NaCl tracer: 100%	Determined, used for sticking efficiency	0.065 m	DM: 0.0084–0.27 NaCl: 0.0171–1.13; [NaCl] = 33 mM CaCl2: 0.1680–1.56; [CaCl2] = 41 mM	Kianfar et al., 2022
	355–425 μm quartz sand	Silica	dsDNA, 80 bp	270 nm	qPCR	10%–83%; NaCl tracer: 100%	2E-3 to 5E-2 min^{-1}	15 cm	0.009–0.22	Chakraborty et al., 2022

	Quartz sand	Protection	DNA tracer used	Size	Detection	encDNA mass recovered	Sorption or attachment	Distance traveled	Sticking efficiency	Reference
Injection into aquifer	Borehole to borehole test in a gravel aquifer	Polymer cage	60–80 nt (ss?DNA)	20–200 nm diameter	qPCR	n.d.	n.d.	3.5 m	n.d.	Garnett et al., 2009
	Injection in sandy gravel (German: Thurtalschotter)	Silica	SiDNASi, dsDNA, 76–120 bp	141–159 nm	qPCR	RB: 104%–123%	n.d.	3 m	n.d.	Kong et al., 2018
	Small hillslope	PLGA	PLGA-dsDNA, 97–96 bp	DLS: 60–930 nm (dependent upon TPGS concentration)	qPCR	n.d.	n.d.	3–5 m	n.d.	McNew et al., 2018
	Fracture-dominated crystalline rock mass	Silica	SiDNASi, dsDNA, 65–120 bp (7 tracers)	166 nm	qPCR	0.04%–44%; Uranine/Sulforhodamine B: 4.9%–70%	n.d.	6.5–37 m	n.d.	Kitila et al., 2019
	Silt loam	PLGA	PLGA-ss?DNA, 87 nt (same as Sharma et al., 2012, Dahlke et al., 2015; McNew et al., 2018)	Not mentioned	qPCR	n.d.	n.d.	5–13 m	n.d.	Georgakakos et al., 2019
	Alluvial gravel aquifer	Alginate	DNA-chitosan coated with alginate, dsDNA, 352 bp	312 ± 132 nm	qPCR	RB (at 21 m): ~0.0001%–0.0003%	n.d.	21–87 m	n.d.	Pang et al., 2020

Note: Mass recovery: encDNA mass recovery compared to mass injected; relative mass recovery (RB): encDNA mass recovery compared to mass recovery of a conservative tracer.
Abbreviations: ds, double stranded; n.d., not determined; RB, relative mass recovery; ss, single stranded.

~4–50% in case CaCl2 type water was used. Furthermore, Kianfar et al. (2022) determined sticking efficiencies, which were relatively high, indicating substantial mass loss.

For encDNA injected into aquifers, mass recoveries ranged from 0.0001% to 85.9%, covering a wide range of recoveries. The recorded travel distances were in the range of 3–87 m for experiments primarily conducted in sandy gravel aquifers or fracture dominated rock. It appeared the alginate covered encDNA particles had overall lower relative mass recoveries than the silica covered encDNA particles, but this could well have been due to the choice of aquifer and size of encapsulated DNA (Pang et al., 2020).

3.3 | Comparing mass balance recoveries

When comparing the mass balance recoveries of dissolved artDNA and encDNA injection experiments (see Figure 3), it is evident that the (relative) mass recoveries per study (indicated by error bars in Figure 3) and between studies ranged considerably, and were almost always less than 100%. The differences in (relative) mass recoveries between dissolved artDNA and encDNA appeared to be relatively limited. However, the range of maximum dissolved artDNA mass recoveries was, except for the glass bead experiments carried out by Zhang et al. (2021), always less than 100%, while, in case of encDNA, Pang et al. (2020), Tang et al. (2021), and Kong et al. (2018) were all able to fully recover the injected encDNA mass. In the cases of Pang et al. and Tang et al., the full recovery experiments were conducted using surface water, while Kong et al. utilized a highly permeable alluvial fill. As mentioned earlier, Pang et al. (2020) and Dahlke et al. (2015), who compared dissolved artDNA and encDNA, concluded that for surface water and wastewater environments the encDNA (relative) mass recovery was higher than dissolved artDNA. Pang et al. (2020), however, concluded that in aquifers encDNA was more subject to filtration removal than dissolved artDNA, so their encDNA was not the first choice to be injected in subsurface media.

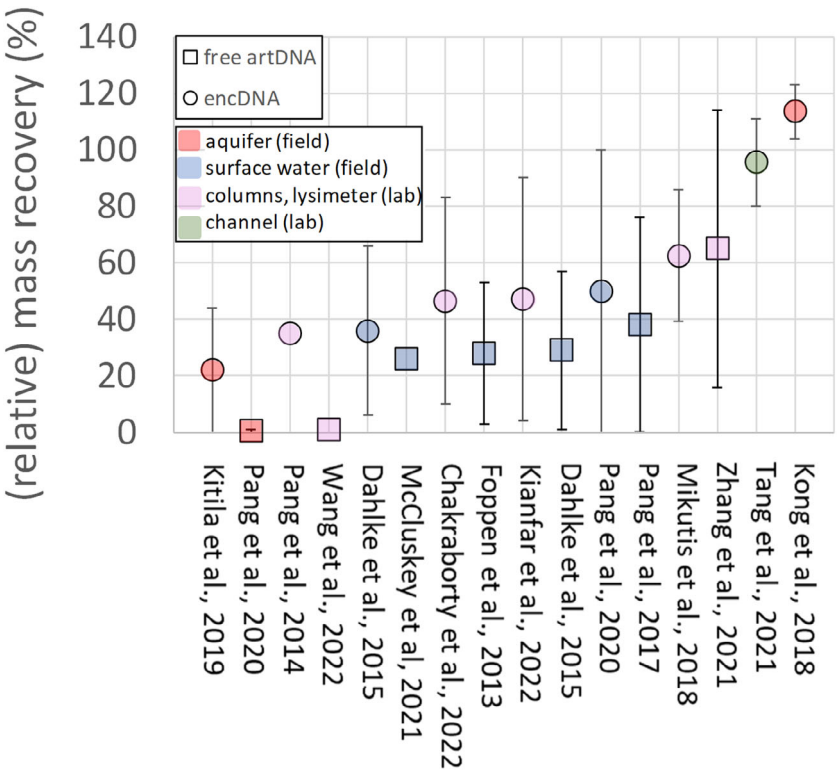

FIGURE 3 Experimentally determined (relative) mass recoveries of dissolved artDNA and encDNA injection experiments in aquifers, surface water, columns, lysimeters, and channels from literature (indicated in color codes). Per study all experimentally determined (relative) mass recoveries of either dissolved artDNA or encDNA were averaged. Bars indicate the minimum and maximum (relative) mass recovery variation per study. In case only one mass recovery was reported bars are missing.

Finally, there was no factor or set of factors controlling mass recovery values. In Figure 3 mass recoveries were given a color. From the colors it was clear that mass recoveries ranged from less than 1%–100% in surface waters, aquifers, columns and lysimeters and open channels in the laboratory.

4 | MASS BALANCE COMPONENTS EXPLAINED

The loss of DNA, either dissolved or encapsulated, in the experiments discussed above was attributed to several factors, with the most significant being instantaneous losses, adsorption or attachment, and decay [e.g., Zhang and Huang (2022)]. The following provides an overview of the processes underlying these sink and source terms in the DNA mass balance. Additionally, where applicable, general mass balance descriptions are given.

4.1 | Adsorption and aggregation in surface water

The surface water injection experiments conducted by Pang et al. (2020) took at most 100 min, and in all cases dissolved artDNA mass recoveries were 1% or less. Subsequently, Pang et al. (2022) clarified that the loss of DNA could be partially attributed to its adsorption to sediment present in the stream, based on static adsorption batch tests. Moreover, the adsorption of DNA in batch tests using effluent was much lower than in identical tests without effluent. Pang et al. (2022) concluded that the DNA tracers may have been competing with similarly charged organic matter for adsorption sites. Also, Dahlke et al. (2015) reported that DNA mass losses in their case could have been due to adsorption to clay particles. Tang et al. (2021) observed the interaction between silica coated artDNA and particulate matter in the stream water they used, as indicated by the irregular breakthrough behavior of encDNA as a function of water quality complexity, which was attributed to the discrete nature of colloidal particles and minor shear-induced aggregation behavior.

Under neutral pH conditions, the phosphate-deoxyribose backbone of DNA (Figure 1) is negatively charged (Bylemans et al., 2018; Greaves & Wilson, 1969; Khanna & Stotzky, 1992; Mauvisseau et al., 2022; Paget et al., 1992; Pietramellara et al., 2002; Pietramellara et al., 2007; Pietramellara et al., 2009). Consequently, positively charged surfaces are electrostatically attracted to DNA, while negatively charged surfaces repel. However, adsorption of negatively charged DNA to negative surfaces also occurs. Recent literature suggests that the adsorption of negatively charged DNA to a negatively charged silica surface can be described by the multicomponent cooperative adsorption model (Moreau model; (Moreau et al., 1991)), or cooperative Langmuir adsorption (Bag et al., 2020; Bag et al., 2021). This implies that DNA binding to silica can only occur in the presence of one or more positively charged binding agents (Bag et al., 2021), such as divalent ions, like Ca^{2+} and Mg^{2+} (Morales-Garcia et al., 2021). In order to mimic environmental conditions, Zhai et al. (2019) studied DNA adsorption in the presence of proteins and polysaccharides in various solution chemistries on a mica (essentially a silica) surface and found that binding strengths of DNA to mica, determined with atomic force microscopy, were higher for Mg^{2+} than for Ca^{2+}, while Cd^{2+} and Ca^{2+} binding strengths were similar. Also, the rather limited binding strengths suggested a noncovalent type of binding of the DNA to the mica surface (Zhai et al., 2019), which aligns with the cooperative Langmuir model. Zhai et al. (2019) also observed that the binding energy of DNA bound to a protein (bovine serum albumin or BSA) to mica was higher than binding of DNA to mica alone, whereas the binding of DNA bound to a polysaccharide (alginate in this case), which was subsequently adsorbed onto mica, was lower. The environmental implication of the findings by Zhai et al. (2019) is that DNA binding to silica surfaces is likely highest or strongest in the presence of proteins in an Mg^{2+} rich environment. Another study of interest is the work of Xue and Feng (2018), who looked at the adsorption and desorption of two types of DNA on two types of sediment for various solution chemistries. They employed NaCl and phosphate buffer for the desorption of DNA from sediments, with the former assumed to extract DNA that was ionically or electrostatically bound, while the latter was used to extract DNA that was ligand-bound. Xue and Feng (2018) found that more DNA was bound by ligand bonds than by electrostatic bonds. With the work of Zhai et al. (2019), Morales-Garcia et al. (2021) and Bag et al. (2021) in mind, it is tempting to interpret these desorption findings in an electrostatic framework of (1) nanoscale charge heterogeneity, whereby mineral surfaces may contain positive charges (Gao et al., 2018; Johnson, 2020; Trauscht et al., 2015) to which negatively charged DNA can attach, and (2) multicomponent cooperative adsorption for like-charged surfaces as described above. Binding is likely entirely electrostatic, but with different binding forces or energies.

With regard to the interaction of DNA and organic matter, Nguyen and Chen (2007) found that DNA adsorption to organic matter occurred when Ca^{2+} and Mg^{2+} were present, while the presence of Na^{+} was found to be insignificant on DNA sorption behavior. In the presence of these cations, Nguyen and Chen (2007) postulated that phosphate groups of DNA and carboxyl groups of NOM would bridge. For a DNA-silica surface system, Nguyen and Elimelech (2007) found that adsorption of DNA to NOM was electrostatically dominated. In this case, adsorption took place at moderately high Na concentrations. Furthermore, DNA adsorption appeared to be irreversible, as DNA release, upon lowering the ionic strength of the solution, did not occur. Peng et al. (2022) looked at the interactions of Suwannee River humic acid (SRHA) and a humic acid from a jar and single stranded DNA (ssDNA). They revealed that non-covalent so-called π-π interactions [related to stacking geometry of aromatic rings; e.g., Bootsma et al., 2019; Thakuria et al., 2019] and divalent cation bridging were the major ssDNA-NOM interaction mechanisms. When Ca^{2+} was available, the humic acid from the jar could completely shield the ssDNA, while this was not the case for SRHA. Peng et al. (2022) hypothesize the differences in shielding are due to differences in aromaticity of NOM, whereby the humic acid from the jar was more aromatic than SRHA. Such NOM-ssDNA interactions may lead to low recovery (amplification inhibition of target DNA during qPCR) and unprecise ssDNA detection (Foppen et al., 2013; Liao et al., 2018; Pang et al., 2020). In hindsight, the instantaneous losses observed in the batch experiments by Foppen et al. (2013) could have been well caused by a combination of Ca^{2+} ions and NOM-ssDNA interactions, potentially leading to the shielding of the DNA molecule and ultimately resulting in low ssDNA detection. Finally, co-solutes like dissolved organic matter or phosphate may compete with DNA, being a biopolymer and colloidal particle, for adsorption sites on particle surfaces, thereby reducing DNA adsorption. The reduction of colloid retention in the presence of organic matter has been well described in the literature (Cheng & Saiers, 2015; Kretzschmar et al., 1995; Morales et al., 2011; Yang et al., 2015).

The adsorption of DNA, either dissolved or encapsulated, onto another particle in surface water, can be called aggregation, which can be conceptually explained by the DLVO theory (e.g., Petosa et al. (2010)). Aggregation can be occur between identical colloids, known as homo-aggregation, or between different colloids (different in size, shape, material, etc.), referred to as hetero-aggregation. Mathematically, the aggregation process can be described as follows:

$$\frac{\partial n_k}{\partial t} = \left[\sum_{i+j=k} \alpha_{ij}\eta_{ij}n_i n_j\right] - \left[n_k \sum_{all\ i} \alpha_{ik}\eta_{ik}n_i\right] \tag{1}$$

whereby n_k is the number concentration of aggregate k, α_{ij} sticking efficiency of smaller particles i and j, η_{ij} collision efficiency of smaller particles i and j, n_i number concentration of particle i, n_j number concentration of particle j, α_{ik} sticking efficiency of particle i and aggregate k, η_{ik} collision efficiency of particle i and aggregate k. In words, Equation (1) describes a particle number mass balance whereby the rate of change of number concentration of k aggregates is equal to the rate of increase of k particles due to aggregation of smaller particles i and j plus the rate of decrease in concentration of k particles due to aggregation of k aggregate with any other particle. Essentially, Equation (1) is the Smoluchowski equation (Smoluchowski, 1917) which, until today, remains the fundamental theory of flocculation (Benjamin, 2013). The collision efficiency for colloids in surface water, η, can be determined from (Praetorius et al., 2020):

$$\eta_{ij} = \frac{2K_B T_W \left(r_i + r_j\right)^2}{3\mu_W r_i r_j} + \frac{4}{3}G\left(r_i + r_j\right)^3 + \pi\left(r_i + r_j\right)^2 \left|v_{s,i} - v_{s,j}\right| \tag{2}$$

where K_B is the Boltzmann constant, T_W water temperature, μ_W viscosity of water, r_i and r_j are the radii of particles or aggregates i and j, respectively, G is the shear rate, and $v_{s,i}$ and $v_{s,j}$ are the settling velocities of particles i and j (Praetorius et al., 2020). Brownian motion collisions are described by the first term in Equation (2), shear forces are described by the second term, and differential sedimentation collisions caused by the differing settling velocities of the particles are described by the last term in the equation. Values of average shear rate in water are $\sim 50–100\ s^{-1}$ (Elimelech et al., 1995). The product of sticking efficiency and collision efficiency in surface water is usually called the aggregation rate. The sticking efficiency, in Equation (1) is defined as the fraction of colliding colloids that stick to each other or aggregate. In case of favorable conditions in terms of charge, $\alpha \approx 1$, and all colliding colloids stick or aggregate. In DLVO terms, there is no energy barrier; only a primary energy minimum due to VDW forces. In case of unfavorable conditions, $\alpha < 1$, and only some fraction of colliding colloids aggregates. In contrast to the collision efficiency, there

has not been a theoretical or approximation method to quantify the sticking efficiency in surface waters. The most common way to arrive at a sticking efficiency for a colloidal suspension in a surface water body of certain chemical quality and suspended matter is experimentally. According to Afrooz et al. (2014), Gallego-Urrea et al. (2011), Labille et al. (2015), Petosa et al. (2010), Praetorius et al. (2014), aggregate rates and sticking efficiency values are typically calculated by tracking particle size over time using Dynamic Light Scattering (DLS), laser diffraction (LD), or nanoparticle tracking analysis, or by following settling of aggregates via batch methods (Barton et al., 2014; Geitner et al., 2017; Tang et al., 2023). In case of hetero-aggregation including sedimentation of hetero-aggregates to the stream bed, then Equations (1) and (2) [e.g., (Benjamin, 2013)] need to be extended, which is beyond the scope of this review.

4.2 | Attachment and detachment in subsurface media

Of all the studies conducted on dissolved artDNA column experiments, Zhang et al. (2021) were the only ones fitting artDNA breakthrough curves, and were able to describe retention using a one-site kinetic attachment and detachment rate coefficient. This finding is significant as it demonstrates that the transport of dissolved artDNA, although a biopolymer, exhibits characteristics similar to colloidal particles. Furthermore, Wang et al. (2022) showed that for their tetra filled sloping lysimeter, the two-site kinetic sorption model proposed by Schijven and Simunek for modeling of viral transport might be used to characterize transient saturation dissolved artDNA transport (Schijven & Šimůnek, 2002). For encDNA injected into columns, transport could be described by a first order kinetic attachment and detachment model, with most of the attachment occurring in the secondary energy minimum, as determined by Kianfar et al., (2022). Depending on the solution chemistry, Kianfar et al. (2022) identified a set of sticking efficiencies, ranging from 8.4E-3 to 1.56. In NaCl and $CaCl_2$ type waters, the majority of particles colliding with the collector surface would also stick to that surface. Chakraborty et al. (2022) also described retention using a one-site kinetic attachment and detachment rate coefficient. Additionally, they showed that with increasing C0, the attachment rate decreased, which was due to interaction of deposited and aqueous phase colloids.

Different modeling strategies are employed to represent the molecular (such as solute) and colloidal transport processes in saturated porous media. (Molnar et al., 2015). Colloids display very restricted diffusive (=Brownian) motion and mostly predictable trajectories, in contrast to solutes, which have a somewhat chaotic motion and lack deterministic trajectories (Molnar et al., 2015). There are over 10 different Colloid Filtration Theories (CFT) or models that simulate these deterministic trajectories and assess the likelihood of colloids reaching collector surfaces (Molnar et al., 2015). Analogous to surface water, most CFTs for porous media comprise two main components: (1) a model that describes colloid trajectory and attachment, and (2) correlation equation(s) that usually includes many variables, which then approximate(s) the results of the mechanistic model. This allows for the prediction of transport. The most important one of those models parameter is the collector contact efficiency, η, defined as the fraction of colloids able to contact the collector in a given system (Molnar et al., 2015). Without going into much detail regarding the various models that describe colloid trajectory and attachment (see Molnar et al. (2015) for an overview), in the majority of CFTs, interception, gravitational sedimentation, and Brownian diffusion are commonly used to explain how colloids are transported from the pore fluid to the area around a filter grain (collector) (Tufenkji, 2004).

When a particle traveling down a streamline collides with a collector because of its size, interception takes place. The settling of particles onto the collector surface with densities larger than the fluid is referred to as gravitational sedimentation. Brownian motion (diffusion) is effective for smaller particles, which causes them to contact collector grains (Tufenkji and Elimelech, 2004). These processes are taken into consideration by the predictive correlation equation, which has been widely used to forecast the deposition (filtration) of colloidal particles in porous media (Tufenkji and Elimelech, 2004):

$$\eta_0 = 2.4A_s^{1/3}N_R^{-0.081}N_{Pe}^{-0.715}N_{\mathrm{vdW}}^{0.052} + 0.55A_S N_R^{1.675}N_A^{0.125} + 0.22N_R^{-0.24}N_G^{1.11}N_{\mathrm{vdW}}^{0.053} \quad (3)$$

whereby η_0 is the single collector contact efficiency, N_R is the aspect ratio, N_{Pe} is a Peclet number characterizing the ratio of convective over diffusive transport, N_{vdW} characterizes the ratio of van der Waals interaction energy to the particle's thermal energy, N_{gr} is a measure for the gravitational potential of the particle, N_A represents the combined influence of Van der Waals attraction forces and fluid velocity on the particle deposition rate due to interception, and, finally N_G is the ratio of Stokes particle settling velocity to approach velocity of the fluid. Equation (3) does not include

ionic strength nor does it include characteristic features of the DLVO theory (energy minima and barrier). Research shows that under favorable conditions, that is when the charge of colloid and collector surface or colloid are opposing and there is no energy barrier to reach the primary minimum as predicted by the DLVO theory, transport can indeed be predicted using such correlation equation (Molnar et al., 2015). In case of unfavorable attachment, that is when the charge of colloid and collector surface or colloid have a similar sign, and the colloid is able to overcome the energy barrier and reaches the primary minimum, the correlation equation has little predictive value. Since most surfaces in the natural environment are negatively charged including DNA tracer surfaces, it is because of these unfavorable conditions difficult to predict DNA tracer transport. Deposition on the solid surface can then be described by first order rate kinetics:

$$\frac{\rho_b}{\theta}\frac{\partial S}{\partial t} = k_a \mathrm{C} \tag{4}$$

where k_a is the colloid deposition rate coefficient, which is related to the single-collector removal efficiency like the one defined in Equation (3) via (Tufenkji, 2004):

$$k = \frac{3(1-\theta)v}{2d_c}\eta_0\alpha \tag{5}$$

where d_c is the diameter of the collector grains, and α is—again—the sticking efficiency, which was already earlier defined as the fraction of colloids reaching the surface also stick to that surface. The analogy between the colloid deposition rate in saturated porous media and the aggregation rate in surface water systems (see below), both essentially defined by a collision efficiency and a sticking efficiency, is clear. Please note that there are different relationships between k and η depending on the CFT used (Molnar et al., 2015). In case of favorable conditions, $\alpha \approx 1$, and the attachment rate coefficient can be calculated. In case of unfavorable conditions, $\alpha < 1$. Recently, Johnson (2020) proposed a theoretical framework to quantitatively link fundamental physicochemical characteristics to macroscale transport kinetic rate coefficients for unfavorable conditions involving nanoscale heterogeneity and mechanistic pore-scale colloid trajectory simulations. However, so far, the parameter was independently determined with tests like column experiments. Particle transport models for dual deposition mode, single-site deposition and remobilization, dual-site deposition and remobilization, single-site deposition and remobilization and blocking, and so forth, have all been proposed in the literature [see e.g., Goldberg et al. (2014)].

4.3 | Decay of DNA

Pang et al. (2020) determined decay rate factors of dissolved artDNA ranging from 0.04 to 0.35 day^{-1}, so, assuming a decay rate of 0.34 day^{-1}, loss due to decay within a 2-hour period, and assuming log linearity, would be ~50%. Also, Pang et al. (2020) showed that their K-tracer group's non-amplified flanking areas, which were 23 bp longer than those of their Seq tracer group, may have helped shield the amplified regions from deterioration brought on by the environment. In a more detailed study, Pang et al. (2022) confirmed that the larger non amplified flanking region indeed results in a significantly lower decay rate than it's shorter counterpart (Pang et al., 2022). More in general, flanking regions degrade significantly faster than internal amplicons (Suzuki et al., 1994). Without using flanking regions, Mikutis et al. (2019) reported that the stability of randomly generated DNA sequences was inversely proportional to its sequence length. In other words, the reduction in concentration of a 53 bp DNA strand as a function of time under influence of light or thermal treatment was much lower than the concentration reduction of a 113 bp DNA strand as a function of time. Also, Jo et al. (2017) demonstrated that in case of mitochondrial eDNA, longer eDNA fragments (719 bp) showed higher decay rates than shorter eDNA fragments (127 bp).

Bylemans et al. (2018) reported that experimental eDNA decay data are increasingly being fitted by exponential decay functions, indicating that, regardless of the source organism, eDNA decays according to a first-order kinetic rate constant. However, several investigations also show that the observed eDNA data are best described by two rate constants (Bylemans et al., 2018). Generally, the data show that eDNA decay rate constants rise as temperature rises (Figure 4). The decay rates of eDNA and dissolved artDNA were visually comparable (Figure 4).

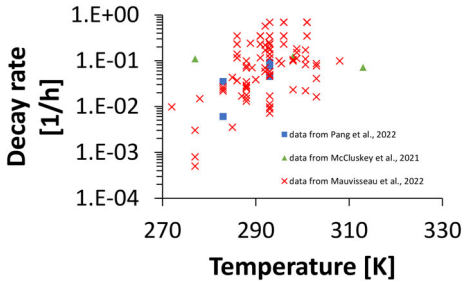

FIGURE 4 Measured DNA decay rate coefficients as a function of temperature in various natural waters. Data from (Mauvisseau et al., 2022) apply to eDNA; data from (Pang et al., 2022) and (McCluskey et al., 2021) apply to dissolved artDNA.

Hydrolysis and oxidation are the two most significant spontaneous biological, chemical, or physical reactions that may change DNA in the environment (Lindahl, 1993; Overballe-Petersen et al., 2013; Zhang et al., 2020). These processes lead to depurination (Wikipedia: "removal of guanine or adenine from a DNA strand") and deamination (Wikipedia: "removal of an amino group from guanine, cytosine or adenine from a DNA strand") of the DNA molecule, resulting in the formation of free DNA fragments in the environment, mostly smaller than 100 base pairs (Overballe-Petersen et al., 2013). DNases catalyze the hydrolysis of DNA (Nishino & Morikawa, 2002), and can be secreted by bacteria (Al-Wahaibi et al., 2019; Kamino & Gulden, 2021). DNAses are found ubiquitously, especially in bodily fluids (Serapinas et al., 2022). Oxidative DNA damage can be induced by reactive oxygen species (ROS; Lee and Kang (2019)). Among all ROS, HO, and O_2 radicals are DNA-reactive species (Dizdaroglu, 2012; Zhang et al., 2020). Due to wet or dry deposition, atmospheric ROS can interact with surface waters (Simões et al., 2021). Moreover, in natural waters ROS can be generated by the photolysis of nitrate, nitrite, hydrogen peroxide (Takeda et al., 2004), and dissolved organic matter (DOM) (Simões et al., 2021; Zhang et al., 2020). Recently, Zhang et al. (2020) proved that when dissolved organic matter was photosensitized, reactive oxygen species were produced, leading to eDNA damage. Another possible process is the physical shearing of DNA molecules. However, Lance et al. (2017) have shown that these forces (due to turbulence) do not play a significant role. This is because the size of DNA is much smaller than the so-called Kolmogorov scale of water (Lance et al., 2017), which is around 0.3–2 mm (Jiménez, 1997). Below this threshold, turbulence is rapidly reduced (Purcel, 1977), thereby leaving eDNA unaffected.

5 | ARTIFICIAL DNA APPLICATION CHALLENGES, USE, AND ECOTOXICITY

5.1 | Challenges

As was pointed out by Liao et al. (2018), the DNA tracer technique offers several advantages: it can be easily distinguishable from environmental background, theoretically unlimited number of tracers, simple to prepare, cost-effective, and environmentally friendly. However, the broader implementation of the DNA multi-tracing technique is still limited and in its early stages, and there are at least two important challenges that need to be overcome. The foremost challenge is the cost associated with producing artDNA. Assuming current prices per base of ∼ € 0,10/base and a cost of ∼€ 20 for a 40 nmol HPLC purification, gives ∼€ 26 for—say—∼35 nmol 60-mer, or 2×10^{16} molecules of artDNA. To provide an indication of the scale in relation to the costs involved, in their experiments, Foppen et al. (2013) injected artDNA masses in the order of 10^{15}–10^{16} molecules and were able to detect at most 10^{10}–10^{12} artDNA molecules per liter 150–650 m away from the injection point in small streams with discharges ranging from 3 to 90 L/s. The detection limit of DNA in a qPCR well is at least some 10 DNA molecules per ∼5 μL sample volume, which equals 2 DNA molecules per 10^{-6} L, or 2×10^6 DNA molecules per liter. So the maximum artDNA concentration of 10^{10} molecules/L Foppen et al. (2013) detected in one of their injection experiments allowed for a 4 log artDNA concentration range in the breakthrough curves, which was similar to the salt tracer concentration range. In other words, the costs of a dissolved artDNA injection experiment are much higher than of a salt tracer injection experiment both yielding similar relative concentration ranges making up the breakthrough curve.

The second challenge lies in the production of encapsulated artDNA particles. Specifically, there is a need to scale up the process, reduce costs, and improve the efficiency of the encapsulation process. Of the encapsulated particles used, the PLA/PLGA particles produced by Sharma et al. (2012) and McNew et al. (2018), the chitosan- alginate particles by Pang et al. (2020), the large PLGA particle produced by Liao et al. (2020), and the silica-DNA-superparamagnetic iron particles used by (Tang et al., 2023) are all still produced at micro- or meso-scale, resulting in limited quantities. However, the silica-DNA-silica particle, originally designed by Paunescu et al. (2013), and used in work of Kianfar et al. (2022); Kittilä et al. (2019); Kong et al. (2018); Mikutis et al. (2018) and (Tang et al., 2021) is since a few years produced on a commercial business-to-business basis by a start-up company in Switzerland. The polymer cage with DNA inside, produced by Garnett et al. (2009) cannot be produced anymore due to unavailability of the required polymers. In terms of efficiencies of the encapsulation process, in case of silica, Paunescu et al. (2013) reported efficiencies of the overall procedure (encapsulation, release and purification) between 25% and 70%. In case of PLGA, McNew et al. (2018) calculated overall efficiencies (encapsulation efficiency times release efficiency) for several different particle preparation procedures in the order of ∼70%. According to McNew et al. (2018) these values were on the high end of literature reported values for the encapsulation of various drugs within PLGA particles. DNA losses in the order of 30%–75% are from a cost point of view not acceptable. Future work should therefore focus on reducing losses by improving DNA encapsulation, release and purification methodologies.

5.2 | How and when to apply artDNA

EncDNA coated with silica has been successfully applied for tracing purposes in various media, including fluids (Bloch et al., 2014; Grass et al., 2014), air (Luescher et al., 2022; Mora et al., 2016), and microbial systems (Mora et al., 2015). In these applications, while mass balances were important, they were not crucial. However, for hydrological applications, mass balance issues of artDNA, either in dissolved form or encapsulated, are significant, and mass recoveries are typically less than 100% (Figure 3). Therefore, when a precise mass balance is required for an injection test, artDNA may not be the ideal choice. However, if complex flow path analyses are the focus, where artDNA with different DNA strands can be injected in multiple locations or added to a source, artDNA is a good candidate. Concrete examples in environmentally oriented hydrological studies include (1) investigating surface water transit times (e.g., in flood storage scenarios), (2) using artDNA as a colloidal surrogate in assessing and predicting movement and dispersion of particulates and pollutants associated with colloids (e.g., bacteria, viruses, radionuclide migration, etc.), (3) studying dynamics in lakes in terms of mixing, and local water mass movements, (4) assessing (preferential) flow paths in saturated and unsaturated zones, (5) understanding connections in groundwater systems, (6) studying water borne sediment movements. Concrete examples in more engineering hydrology approaches include: (1) detecting leaks, for example, in hydraulic structures, groundwater wells, pipelines, and so forth, (2) determining flow direction, velocity, permeability, or locating fractures using single borehole or two-well techniques.

The scale at which artDNA is applied depends on the mass of artDNA that is used. If sufficient artDNA is available there is no theoretical limit to the experimental scale: artDNA masses used are always low (gram scale at most), can be easily carried, and injection is simple and straightforward. This could become an important advantage over the use of a salt tracer, which is limited in application due to the large masses of salt required for large-scale experiments. However, as mentioned earlier, the practical artDNA limit is in the costs of manufacturing artDNA and therefore the scale at which it is applied.

5.3 | Ecotoxicity of artDNA

Although artDNA is a natural biopolymer composed of nontoxic and biodegradable elements, its application in the environment can still be a topic of controversy. There is no proof that any species of flora or wildlife are hazardous to DNA (Lorenz & Wackernagel, 1994; Nielsen et al., 2007). In fact, many species commonly see the phosphorus in extracellular DNA found in aquatic conditions as a food source (e.g., (Dell'Anno & Danovaro, 2005; Siuda et al., 1998). Spontaneous transformation, which occurs when extracellular DNA is incorporated into the genetic makeup of naturally existing bacteria, is believed to be a significant mechanism of horizontal gene transfer (Braus et al., 2022). The incorporation of free DNA into the recipient organism's genome through homologous recombination is a key process in this context (Kung et al., 2013). The minimum length of sequence homology required for successful recombination may

vary significantly depending on the organism and the recombination pathway being employed (Kung et al., 2013). For instance, effective recombination has been observed in Escherichia coli with as little as 23 bp of sequence homology (Huang, 1986). For dissolved artDNA used in environmental applications, transformation seems possible, but—at the same time—chances seem low, because successful transformation is limited if sequence homology is minimized. Most workers that used dissolved artDNA avoided any sequence homology by checking their artDNA nucleotide composition during the experimental design phase with BLAST, as discussed before. Also, in case of dissolved artDNA, the number of molecules applied in tests in the environment usually was limited to $\sim 10^{16}$ molecules or less, which disappear due to decay in a matter of days. When DNA material is prepared from plasmids (e.g., Pang et al., 2020), it is necessary to ensure that the artDNA is plasmid-free to prevent potential horizontal gene transfer. This can be achieved by cleaving the plasmids using restriction enzymes (Nathans & Smith, 1975).

For silica encapsulated DNA particles, Koch et al. (2021) assessed the ecotoxicity of sub-micron silica particles (60, 200, and 1200 nm diameter) with and without encapsulated DNA. Mobility was unaffected by acute toxicity studies on *Daphnia magna* at values below 300 ppm. Furthermore, long-term ecotoxicological potential with *Ceriodaphnia* species and *Raphidocelis subcapitata* (green algae) had no impact at concentrations associated with actual exposure scenarios. Indeed, it is important to acknowledge that eco-toxicological effects of any particle used in environmental applications cannot be completely ruled out. For example, Ahamed et al. (2021) summarized the ecotoxicological effects from 28 studies involving crystalline and/or amorphous silica nanoparticles in size range ~10 to ~100 nm. The effects observed in these studies ranged from no or negligible cytotoxicity, to minor membrane damage, to promotion of inflammatory processes, elevated oxidative stress, and partial cell death. The variation in observed effects between Koch et al. (2021) and the studies summarized by Ahamed et al. (2021) was mainly stemmed from the broader range of ecotoxicity tests used in the latter, as presented in their overview. Also, crystalline silica is known to be more toxic than amorphous silica, which is considered relatively safe (Kim et al., 2015). The particles used by Koch et al. (2021) were colloidal Stöber-type amorphous silica particles. Furthermore, evidence suggests that particle size plays a crucial role, although there is no consensus on the specific size ranges that typically induce ecotoxicological effects. The toxicity of silica depends on the size and dose of the particles, as well as the cell types exposed to the silica (Kim et al., 2015).

Regarding PLGA nanoparticles in both in-vivo and in-vitro studies, they have shown very little to no toxicity (Mir et al., 2017). However, there is a lack of studies on the ecotoxicity effects of PLGA nanoparticles and the same applies to alginate-chitosan particles, despite the fact that both alginate and chitosan are known to be nontoxic, biodegradable, and biocompatible biopolymers.

6 | RESEARCH DIRECTIONS AND RECOMMENDATIONS

One important research direction highlighted by Pang et al. (2020) is the practical advancement of DNA tracer work. The suggest investing in reducing DNA tracer preparation time, automating sample processing and qPCR, and refining tracer detectability in different hydrological matrices. Furthermore, they mentioned the potential for rapid detection of DNA tracers in the field as portable PCR and qPCR devices become increasingly available (Billington et al., 2021). This advancement would enable more efficient and real-time monitoring of DNA tracers in hydrological systems. Upscaling DNA production, both in free and encapsulated form at a reasonable cost is another practical research direction. This would involve increasing the efficiency of the encapsulation process including the encapsulation itself, release and purification steps. Ideally, the amount of DNA per encapsulate should be tunable or controlled in order to increase the qPCR signal per encapsulate, if necessary.

Secondly, one of the questions and challenges posed by Zhang and Huang (2022) with regard to dissolved artDNA and encDNA in groundwater environments was on resolving adsorption and degradation characteristics. Current review shows that progress has been made. In summary (see also Figure 5): Adsorption of DNA to charged surfaces is predominantly electrostatic, both for attractive and repelling conditions. In the latter case, the multicomponent cooperative adsorption or cooperative Langmuir adsorption should be used, whereby positive binding agents like divalent ions (e.g., Ca and Mg) play a role, but also proteins and polysaccharides. In fact, DNA binding to silica surfaces is likely highest in the presence of proteins in an Mg^{2+} rich environment (Zhai et al., 2019). DNA adsorption to organic matter is due to Ca^{2+} and Mg^{2+}, which bridge phosphate groups of DNA and carboxyl groups of NOM (Nguyen & Chen, 2007). Also, aromaticity of NOM plays a role (Peng et al., 2022). With regard to decay, longer DNA fragments show higher decay rates than shorter DNA fragments. Also, larger non amplified flanking regions of a piece of DNA result in a significantly lower decay rate than it's shorter counterpart (Pang et al., 2022). Furthermore, hydrolysis and

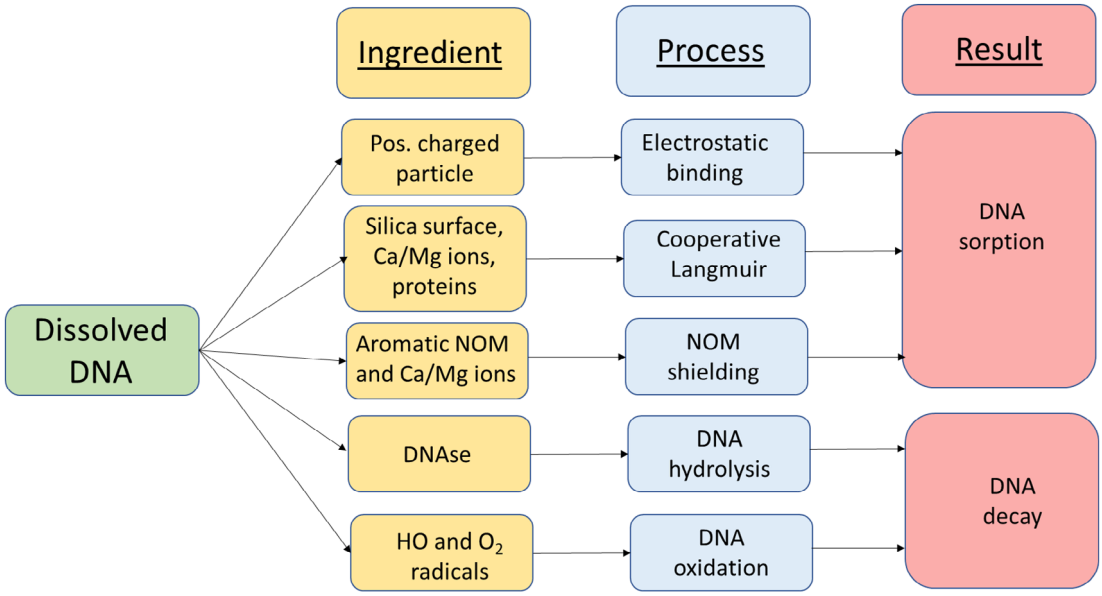

FIGURE 5 Sorption and decay of dissolved DNA. Break-down of ingredients dissolved DNA can collide with in environmental waters and processes occurring upon collision, which lead to either sorption or decay of dissolved DNA.

oxidation are the two most significant reactions that degrade DNA in the environment. The first is catalyzed by DNases, which are found everywhere; the second can be induced by HO and O_2 radicals in water, either originating from atmospheric radicals (Simões et al., 2021) or generated by photolysis of dissolved organic matter (Zhang et al., 2020). Although these processes are known to occur, it does not mean they can already be quantified for a wide range of environmental systems, such that they can be incorporated as a term in the mass balance in order to better understand mass recoveries. Therefore, quantification of DNA adsorption and DNA decay processes remain important research directions.

Thirdly, an important question to address is the arrangement of (bio)molecules at the surface of dissolved artDNA or encDNA. Zhai et al. (2019) have already demonstrated the effect of proteins on dissolved DNA sorption, as discussed earlier. In case of encDNA, these biomolecules may form an environmental corona. Research in marine and freshwater environments found that (nano)particles are quickly coated by natural organic macromolecules (NOM), such as humic and fluvic acids, lipids, polysaccharides, and proteins, producing an environmental corona, after being released into the environment (Galloway et al., 2017; Lynch et al., 2014; Xu et al., 2020; Yang et al., 2013). Xu and workers (Xu et al., 2020) defined four main groups of substances in aquatic ecosystems, each with different effects and/or nanoparticle interaction: proteins, extracellular polymeric substances (EPS), natural organic matter (NOM), and other constituents like surfactants. The hypothesis is that these (bio)polymers will mask the primary energy minimum (e.g., Johnson & Logan, 1996; Yan et al., 2019), enhancing colloidal stability and reducing aggregation with other particles or particulate suspended matter (Lartiges et al., 2001). This corona formation may also reduce attachment to collector surfaces, like sediment grains, potentially reducing DNA attachment and mass loss, thus enhancing its transport and tracer-like capabilities. Additionally, the potential eco-toxicity of nanoparticles can likely be related to the role of an environmental corona, as was pointed out by Xu et al. (2020). There is—still—very limited work carried out on assessing eco-toxicity effects of encDNA. Koch et al. (2021) were the first to do so, and they showed no acute or chronic eco-toxicological effects of silica encapsulated DNA particles. Such work has not yet been carried out for PLGA and alginate encapsulated DNA particles. Nonetheless, Chiu et al. (2021) found a relation between PLGA particle size and cytotoxicity, as measured by the dose required to reduce 50% cell viability. They concluded that in the size range 100–300 nm, the smaller the PLGA particle the higher the cytotoxicity potency was. This finding of Chiu and workers might be indicative of PLGA eco-toxicity for organisms in environmental applications. Another interesting idea is the relation between eco-corona formation and decay of dissolved artDNA. An arrangement of biomolecules surrounding free DNA might shield DNA from DNAses, thereby reducing potential DNA decay.

Although artDNA can be injected at various locations in order to study groundwater or surface water hydraulics of a particular system, up to date, only Kittilä et al. (2019) made use of this unique multi-tracer feature of artDNA so far.

It is recommended to conduct more studies where artDNA is employed to map complex flow paths and source, thereby further assessing the potential and limitations of the technique. A multi-reactive tracer injection scheme could consist of a number of artDNA masses with different nucleotide composition injected in both space and time, injection of both dissolved and encapsulated artDNA, with the aim to identify groundwater flow velocities of faster flowlines, residence times, connections between injection and abstraction or recharge and discharge.

Furthermore, it is advisable to establish a minimum set of components that should ideally be included in a report on DNA injection tests. In addition to comparing breakthrough curves with a salt tracer, the recovered mass of artDNA should be determined, and if possible, the independently measured mass losses should also be reported. It is also recommended to include qPCR dilution curves in the report, including No Template Control (NTC) values, to assess the reliability of the qPCR assay used. These measures will contribute to a more comprehensive evaluation of DNA tracer studies.

7 | CONCLUSIONS

1. In case of dissolved artDNA injected in streams, mass recoveries—if determined—ranged between less than 1% to at most 57% for stretch lengths between 28 and 1192 m. In those cases, mass recoveries of conservative tracer were usually in the order of 90%–100%. So, dissolved artDNA did not behave in the same way as a conservative tracer. Loss of artDNA was due to a variety of factors of which the most important ones were instantaneous losses, sorption onto suspended particles, and decay.
2. In most dissolved artDNA stream injection experiments, the shape of the breakthrough curve in terms of time to rise, time to peak, and dispersion coefficient were visually similar to the breakthrough curve of a conservative tracer.
3. For dissolved artDNA injected into saturated sand or glass bead column experiments, mass recoveries—if determined—ranged from 0.009% to 74%. Only Aquilanti et al. (2013) reported no sorption or removal from which I concluded their artDNA mass recoveries were ~100%. For glass bead columns, Zhang et al. (2021) observed DNA length dependent (90–200 bp) mass recovery, whereby DNA recovery increased with increasing DNA length (80%–114% mass recovery).
4. Retention of dissolved artDNA in saturated sand columns can be described using one-site or two-site kinetic attachment and detachment rate coefficient(s). This showed that transport of dissolved artDNA, although a biopolymer, was typically colloid-like, whereby particle attachment is related to η_0 and α, according to Equation (5).
5. Breakthrough of dissolved artDNA was sometimes earlier than that of a conservative tracer (Aquilanti et al., 2013; McCluskey et al., 2021; Pang et al., 2017; Pang et al., 2020; Ptak et al., 2004; Zhang et al., 2021), but breakthrough could also be significantly retarded Zhang et al. (2021); their sand column tests).
6. For dissolved artDNA injected into aquifers, only Pang et al. (2017) and Pang et al. (2020) determined mass recoveries, which ranged from less than 0.0001%–76%, dependent on aquifer type (in their case: fine coastal sand versus alluvial gravel).
7. In case of encDNA injected into surface waters, mass recoveries of the various encDNA particle types were in the range 6%–111%, which was in general higher than mass recoveries of dissolved artDNA. Both Dahlke et al. (2015) and Pang et al. (2020), who both applied dissolved and encapsulated artDNA in the same experimental setting indeed reported higher mass recoveries for encDNA than for dissolved artDNA.
8. For encDNA injected into columns, transport could be described with first order kinetic attachment and detachment, whereby most of the attachment took place in the secondary energy minimum (Kianfar et al., 2022). Dependent on solution chemistry, Kianfar et al. determined a set of sticking efficiencies, ranging from 8.4E-3 to 1.56, dependent on solution chemistry. This indicated that in NaCl and CaCl2 type waters, most of the silica DNA particles of Kianfar et al. colliding with the collector surface would also stick to that surface.
9. For encDNA injected into aquifers, mass recoveries ranged from 0.0001% to 85.9%, spanning a wide range of recoveries. Recorded traveled distances were in the order of 3–87 m for experiments mostly carried out in sandy gravel aquifers or fracture dominated rock.
10. Research on hydrological applications of dissolved artDNA and encDNA should focus on quantifying artDNA adsorption and decay, the arrangement of biomolecules at the surface of both dissolved artDNA and encDNA in order to alter adsorption and/or decay, and on the practical advancement of DNA tracer work. More in particular, these are reducing DNA tracer preparation time, automating sample processing and qPCR, rapid detection of DNA

tracers in the field, and refining tracer detectability. Furthermore, research should focus on upscaling of DNA production, either protected or unprotected, and increasing the efficiency of the encapsulation process including the encapsulation itself, release and purification steps.

AUTHOR CONTRIBUTIONS

Jan Willem Foppen: Conceptualization (lead); formal analysis (lead); visualization (lead); writing – original draft (lead).

CONFLICT OF INTEREST STATEMENT

The authors declare no conflicts of interest.

DATA AVAILABILITY STATEMENT

Data sharing is not applicable to this article as no new data were created or analyzed in this study.

ORCID

Jan Willem Foppen https://orcid.org/0000-0002-1112-2383

RELATED WIREs ARTICLES

Colloid transport through soil and other porous media under transient flow conditions—A review

REFERENCES

Abbott, B. W., Baranov, V., Mendoza-Lera, C., Nikolakopoulou, M., Harjung, A., Kolbe, T., Balasubramanian, M. N., Vaessen, T. N., Ciocca, F., Campeau, A., Wallin, M. B., Romeijn, P., Antonelli, M., Gonçalves, J., Datry, T., Laverman, A. M., de Dreuzy, J. R., Hannah, D. M., Krause, S., … Pinay, G. (2016). Using multi-tracer inference to move beyond single-catchment ecohydrology. *Earth-Science Reviews*, *160*, 19–42.

Afrooz, A. R. M. N., Hussain, S. M., & Saleh, N. B. (2014). Aggregate size and structure determination of nanomaterials in physiological media: Importance of dynamic evolution. *Journal of Nanoparticle Research*, *16*(12), 2771.

Ahamed, A., Liang, L., Lee, M. Y., Bobacka, J., & Lisak, G. (2021). Too small to matter? Physicochemical transformation and toxicity of engineered nTiO2, nSiO2, nZnO, carbon nanotubes, and nAg. *Journal of Hazardous Materials*, *404*(Pt A, 124107.

Al-Wahaibi, A. S. M., Lapinska, E., Rajarajan, N., Dobretsov, S., Upstill-Goddard, R., & Burgess, J. G. (2019). Secretion of DNases by marine bacteria: A culture based and bioinformatics approach. *Frontiers in Microbiology*, *10*, 969.

Aquilanti, L., Clementi, F., Landolfo, S., Nanni, T., Palpacelli, S., & Tazioli, A. (2013). A DNA tracer used in column tests for hydrogeology applications. *Environmental Earth Sciences*, *70*(7), 3143–3154.

Aquilanti, L., Clementi, F., Nanni, T., Palpacelli, S., Tazioli, A., & Vivalda, P. M. (2016). DNA and fluorescein tracer tests to study the recharge, groundwater flowpath and hydraulic contact of aquifers in the Umbria-Marche limestone ridge (central Apennines, Italy). *Environmental Earth Sciences*, *75*(7). https://doi.org/10.1007/s12665-016-5436-5

Auckenthaler, A., Raso, G., & Huggenberger, P. (2002). Particle transport in a karst aquifer: Natural and artificial tracer experiments with bacteria, bacteriophages and microspheres. *Water Science and Technology*, *46*(3), 131–138.

Bag, S., Rauwolf, S., Schwaminger, S. P., Wenzel, W., & Berensmeier, S. (2021). DNA binding to the silica: Cooperative adsorption in action. *Langmuir*, *37*(19), 5902–5908.

Bag, S., Rauwolf, S., Suyetin, M., Schwaminger, S. P., Wenzel, W., & Berensmeier, S. (2020). Buffer influence on the amino acid silica interaction. *ChemPhysChem*, *21*(20), 2347–2356.

Barton, L. E., Therezien, M., Auffan, M., Bottero, J. Y., & Wiesner, M. R. (2014). Theory and methodology for determining nanoparticle affinity for heteroaggregation in environmental matrices using batch measurements. *Environmental Engineering Science*, *31*(7), 421–427.

Benjamin, M. M., & Lawler, D. F. (2013). *Water quality engineering physical/chemical treatment processes*. JohnWiley & Sons, Inc.

Billington, C., Abeysekera, G., Scholes, P., Pickering, P., & Pang, L. (2021). Utility of a field deployable qPCR instrument for analyzing freshwater quality. *Agrosystems, Geosciences & Environment*, *4*(4), e20223.

Bloch, M. S., Paunescu, D., Stoessel, P. R., Mora, C. A., Stark, W. J., & Grass, R. N. (2014). Labeling milk along its production chain with DNA encapsulated in silica. *Journal of Agricultural and Food Chemistry*, *62*(43), 10615–10620.

Bootsma, A. N., Doney, A. C., & Wheeler, S. E. (2019). Predicting the strength of stacking interactions between heterocycles and aromatic amino acid side chains. *Journal of the American Chemical Society*, *141*(28), 11027–11035.

Braus, S. A. G., Short, F. L., Holz, S., Stedman, M. J. M., Gossert, A. D., & Hospenthal, M. K. (2022). The molecular basis of FimT-mediated DNA uptake during bacterial natural transformation. *Nature Communications*, *13*(1), 1065.

Bylemans, J., Furlan, E. M., Gleeson, D. M., Hardy, C. M., & Duncan, R. P. (2018). Does size matter? An experimental evaluation of the relative abundance and decay rates of aquatic environmental DNA. *Environmental Science & Technology*, *52*(11), 6408–6416.

Chakraborty, S., Foppen, J. W., & Schijven, J. F. (2022). Effect of concentration of silica encapsulated ds-DNA colloidal microparticles on their transport through saturated porous media. *Colloids and Surfaces A: Physicochemical and Engineering Aspects*, *651*, 129625.

Cheng, T., & Saiers, J. E. (2015). Effects of dissolved organic matter on the co-transport of mineral colloids and sorptive contaminants. *Journal of Contaminant Hydrology*, *177-178*, 148–157.

Chiu, H. I., Samad, N. A., Fang, L., & Lim, V. (2021). Cytotoxicity of targeted PLGA nanoparticles: A systematic review. *RSC Advances*, *11*(16), 9433–9449.

Dahlke, H. E., Williamson, A. G., Georgakakos, C., Leung, S., Sharma, A. N., Lyon, S. W., & Walter, M. T. (2015). Using concurrent DNA tracer injections to infer glacial flow pathways. *Hydrological Processes*, *29*(25), 5257–5274.

Dell'Anno, A., & Danovaro, R. (2005). Ecology: Extracellular DNA plays a key role in deep-sea ecosystem functioning. *Science*, *309*(5744), 2179.

Dizdaroglu, M. (2012). Oxidatively induced DNA damage: Mechanisms, repair and disease. *Cancer Letters*, *327*(1–2), 26–47.

Elimelech, M., Gregory, J., Jia, X., & Williams, R. A. (1995). Modelling of particle deposition onto ideal collectors. In M. Elimelech, J. Gregory, X. Jia, & R. A. Williams (Eds.), *Particle deposition & aggregation* (pp. 113–156). Butterworth-Heinemann.

Ettayfi, N., Bouchaou, L., Michelot, J. L., Tagma, T., Warner, N., Boutaleb, S., Massault, M., Lgourna, Z., & Vengosh, A. (2012). Geochemical and isotopic (oxygen, hydrogen, carbon, strontium) constraints for the origin, salinity, and residence time of groundwater from a carbonate aquifer in the Western anti-Atlas mountains, Morocco. *Journal of Hydrology*, *438-439*, 97–111.

Flynn, R. M., & Sinreich, M. (2010). Characterisation of virus transport and attenuation in epikarst using short pulse and prolonged injection multi-tracer testing. *Water Research*, *44*(4), 1138–1149.

Foppen, J. W., Orup, C., Adell, R., Poulalion, V., & Uhlenbrook, S. (2011). Using multiple artificial DNA tracers in hydrology. *Hydrological Processes*, *25*(19), 3101–3106.

Foppen, J. W., Seopa, J., Bakobie, N., & Bogaard, T. (2013). Development of a methodology for the application of synthetic DNA in stream tracer injection experiments. *Water Resources Research*, *49*(9), 5369–5380.

Gallego-Urrea, J. A., Tuoriniemi, J., & Hassellöv, M. (2011). Applications of particle-tracking analysis to the determination of size distributions and concentrations of nanoparticles in environmental, biological and food samples. *TrAC—Trends in Analytical Chemistry*, *30*(3), 473–483.

Galloway, T. S., Cole, M., & Lewis, C. (2017). Interactions of microplastic debris throughout the marine ecosystem. *Nature Ecology and Evolution*, *1*(5), 0116.

Gao, Z., Xie, L., Cui, X., Hu, Y., Sun, W., & Zeng, H. (2018). Probing anisotropic surface properties and surface forces of fluorite crystals. *Langmuir*, *34*(7), 2511–2521.

Garnett, M. C., Ferruti, P., Ranucci, E., Suardi, M. A., Heyde, M., & Sleat, R. (2009). Sterically stabilized self-assembling reversibly cross-linked polyelectrolyte complexes with nucleic acids for environmental and medical applications. *Biochemical Society Transactions*, *37*(4), 713–716.

Geitner, N. K., O'Brien, N. J., Turner, A. A., Cummins, E. J., & Wiesner, M. R. (2017). Measuring nanoparticle attachment efficiency in complex systems. *Environmental Science and Technology*, *51*(22), 13288–13294.

Goeppert, N., & Goldscheider, N. (2019). Improved understanding of particle transport in karst groundwater using natural sediments as tracers. *Water Research*, *166*, 115045.

Georgakakos, C. B., Richards, P. L., & Walter, M. T. (2019). Tracing septic pollution sources using synthetic DNA tracers: proof of concept. *Air, Soil and Water Research*, *12*, 117862211986379. https://doi.org/10.1177/1178622119863794

Goldberg, E., Scheringer, M., Bucheli, T. D., & Hungerbühler, K. (2014). Critical assessment of models for transport of engineered nanoparticles in saturated porous media. *Environmental Science and Technology*, *48*(21), 12732–12741.

González-Pinzõn, R., Haggerty, R., & Dentz, M. (2013). Scaling and predicting solute transport processes in streams. *Water Resources Research*, *49*(7), 4071–4088.

Grass, R. N., Schälchli, J., Paunescu, D., Soellner, J. O. B., Kaegi, R., & Stark, W. J. (2014). Tracking trace amounts of submicrometer silica particles in wastewaters and activated sludge using silica-encapsulated DNA barcodes. *Environmental Science and Technology Letters*, *1*(12), 484–489.

Greaves, M. P., & Wilson, M. J. (1969). The adsorption of nucleic acids by montmorillonite. *Soil Biology and Biochemistry*, *1*(4), 317–323.

Huang, P. S.a. H. V. (1986). Homologus recombination in *Escherichia Coli*—Dependence on substrate length and homology. *Genetics*, *112*, 441–457.

Jiménez, J. (1997). Oceanic turbulence at millimeter scales. *Scientia Marina*, *61*(Suppl.1), 47–56.

Jo, T., Murakami, H., Masuda, R., Sakata, M. K., Yamamoto, S., & Minamoto, T. (2017). Rapid degradation of longer DNA fragments enables the improved estimation of distribution and biomass using environmental DNA. *Molecular Ecology Resources*, *17*(6), e25–e33.

Johnson, W. P. (2020). Quantitative linking of nanoscale interactions to continuum-scale nanoparticle and microplastic transport in environmental granular media. *Environmental Science & Technology*, *54*(13), 8032–8042.

Johnson, W. P., & Logan, B. E. (1996). Enhanced transport of bacteria in porous media by sediment-phase and aqueous-phase natural organic matter. *Water Research*, *30*(4), 923–931.

Kamino, L. N., & Gulden, R. H. (2021). The effect of crop species on DNase-producing bacteria in two soils. *Annals of Microbiology*, *71*(1), 14.

Khanna, M., & Stotzky, G. (1992). Transformation of Bacillus subtilis by DNA bound on montmorillonite and effect of DNase on the transforming ability of bound DNA. *Applied and Environmental Microbiology*, *58*(6), 1930–1939.

Kianfar, B., Tian, J., Rozemeijer, J., van der Zaan, B., Bogaard, T. A., & Foppen, J. W. (2022). Transport characteristics of DNA-tagged silica colloids as a colloidal tracer in saturated sand columns; role of solution chemistry, flow velocity, and sand grain size. *Journal of Contaminant Hydrology*, *246*, 103954.

Kim, I. Y., Joachim, E., Choi, H., & Kim, K. (2015). Toxicity of silica nanoparticles depends on size, dose, and cell type. *Nanomedicine*, *11*(6), 1407–1416.

Kirchner, J. W. (2016a). Aggregation in environmental systems-Part 1: Seasonal tracer cycles quantify young water fractions, but not mean transit times, in spatially heterogeneous catchments. *Hydrology and Earth System Sciences*, *20*(1), 279–297.

Kirchner, J. W. (2016b). Aggregation in environmental systems-Part 2: Catchment mean transit times and young water fractions under hydrologic nonstationarity. *Hydrology and Earth System Sciences*, *20*(1), 299–328.

Kittilä, A., Jalali, M. R., Evans, K. F., Willmann, M., Saar, M. O., & Kong, X. Z. (2019). Field comparison of DNA-labeled nanoparticle and solute tracer transport in a fractured crystalline rock. *Water Resources Research*, *55*(8), 6577–6595.

Koch, J., Doswald, S., Mikutis, G., Stark, W. J., & Grass, R. N. (2021). Ecotoxicological assessment of DNA-tagged silica particles for environmental tracing. *Environmental Science and Technology*, *55*(10), 6867–6875.

Kong, X. Z., Deuber, C. A., Kittilä, A., Somogyvári, M., Mikutis, G., Bayer, P., Stark, W. J., & Saar, M. O. (2018). Tomographic reservoir imaging with DNA-labeled silica nanotracers: The first field validation. *Environmental Science and Technology*, *52*(23), 13681–13689.

Kretzschmar, R., Robarge, W. P., & Amoozegar, A. (1995). Influence of natural organic matter on colloid transport through saprolite. *Water Resources Research*, *31*(3), 435–445.

Kung, S. H., Retchless, A. C., Kwan, J. Y., & Almeida, R. P. (2013). Effects of DNA size on transformation and recombination efficiencies in Xylella fastidiosa. *Applied and Environmental Microbiology*, *79*(5), 1712–1717.

Labille, J., Harns, C., Bottero, J. Y., & Brant, J. (2015). Heteroaggregation of titanium dioxide nanoparticles with natural clay colloids. *Environmental Science and Technology*, *49*(11), 6608–6616.

Lance, R., Klymus, K., Richter, C., Guan, X., Farrington, H., Carr, M., Thompson, N., Chapman, D., & Baerwaldt, K. (2017). Experimental observations on the decay of environmental DNA from bighead and silver carps. *Management of Biological Invasions*, *8*(3), 343–359.

Lartiges, B. S., Deneux-Mustin, S., Villemin, G., Mustin, C., Barrès, O., Chamerois, M., Gerard, B., & Babut, M. (2001). Composition, structure and size distribution of suspended particulates from the Rhine River. *Water Research*, *35*(3), 808–816.

Lee, T. H., & Kang, T. H. (2019). DNA oxidation and excision repair pathways. *International Journal of Molecular Sciences*, *20*(23), 6092.

Leibundgut, C., Maloszewski, P. and Külls, C. (2009) Tracers in hydrology.

Liao, R., Yang, P., Wu, W., Luo, D., & Yang, D. (2018). A DNA tracer system for hydrological environment investigations. *Environmental Science and Technology*, *52*(4), 1695–1703.

Liao, R., Zhang, J., Li, T., Luo, D., & Yang, D. (2020). Biopolymer/plasmid DNA microspheres as tracers for multiplexed hydrological investigation. *Chemical Engineering Journal*, *401*, 126035.

Lindahl, T. (1993). Instability and decay of the primary structure of DNA. *Nature*, *362*(6422), 709–715.

Lorenz, M. G., & Wackernagel, W. (1994). Bacterial gene transfer by natural genetic transformation in the environment. *Microbiological Reviews*, *58*(3), 563–602.

Luescher, A. M., Koch, J., Stark, W. J., & Grass, R. N. (2022). Silica-encapsulated DNA tracers for measuring aerosol distribution dynamics in real-world settings. *Indoor Air*, *32*(1), e12945.

Lynch, I., Dawson, K. A., Lead, J. R., & Valsami-Jones, E. (2014). Macromolecular coronas and their importance in nanotoxicology and nanoecotoxicology. *Frontiers of Nanoscience*, *7*, 127–156.

Mauvisseau, Q., Harper, L. R., Sander, M., Hanner, R. H., Kleyer, H., & Deiner, K. (2022). The multiple states of environmental DNA and what is known about their persistence in aquatic environments. *Environmental Science & Technology*, *56*(9), 5322–5333.

McCluskey, J., Flores, M. E., Hinojosa, J., Jafarzadeh, A., Moghadam, S. V., Phan, D. C., Green, R. T., & Kapoor, V. (2021). Tracking water with synthetic DNA tracers using droplet digital PCR. *ACS ES&T Water*, *1*(5), 1177–1183.

McDonnell, J. J., & Beven, K. (2014). Debates— The future of hydrological sciences: A (common) path forward? A call to action aimed at understanding velocities, celerities and residence time distributions of the headwater hydrograph. *Water Resources Research*, *50*(6), 5342–5350.

McNew, C. P., Wang, C., Walter, M. T., & Dahlke, H. E. (2018). Fabrication, detection, and analysis of DNA-labeled PLGA particles for environmental transport studies. *Journal of Colloid and Interface Science*, *526*, 207–219.

Mikutis, G., Deuber, C. A., Schmid, L., Kittilä, A., Lobsiger, N., Puddu, M., Asgeirsson, D. O., Grass, R. N., Saar, M. O., & Stark, W. J. (2018). Silica-encapsulated DNA-based tracers for aquifer characterization. *Environmental Science and Technology*, *52*(21), 12142–12152.

Mikutis, G., Schmid, L., Stark, W. J., & Grass, R. N. (2019). Length-dependent DNA degradation kinetic model: Decay compensation in DNA tracer concentration measurements. *AICHE Journal*, *65*(1), 40–48.

Mir, M., Ahmed, N., & Rehman, A. U. (2017). Recent applications of PLGA based nanostructures in drug delivery. *Colloids and Surfaces. B, Biointerfaces*, *159*, 217–231.

Molnar, I. L., Johnson, W. P., Gerhard, J. I., Willson, C. S., & O'Carroll, D. M. (2015). Predicting colloid transport through saturated porous media: A critical review. *Water Resources Research*, *51*(9), 6804–6845.

Mora, C. A., Paunescu, D., Grass, R. N., & Stark, W. J. (2015). Silica particles with encapsulated DNA as trophic tracers. *Molecular Ecology Resources*, *15*(2), 231–241.

Mora, C. A., Schärer, H. J., Oberhänsli, T., Ludwig, M., Stettler, R., Stoessel, P. R., Grass, R. N., & Stark, W. J. (2016). Ultrasensitive quantification of pesticide contamination and drift using silica particles with encapsulated DNA. *Environmental Science and Technology Letters*, *3*(1), 19–23.

Morales, V. L., Zhang, W., Gao, B., Lion, L. W., Bisogni, J. J., Jr., McDonough, B. A., & Steenhuis, T. S. (2011). Impact of dissolved organic matter on colloid transport in the vadose zone: Deterministic approximation of transport deposition coefficients from polymeric coating characteristics. *Water Research*, *45*(4), 1691–1701.

Morales-Garcia, A. L., Walton, R., Blakeman, J. T., Banwart, S. A., Harding, J. H., Geoghegan, M., Freeman, C. L., & Rolfe, S. A. (2021). The role of extracellular DNA in microbial attachment to oxidized silicon surfaces in the presence of Ca(2+) and Na(). *Langmuir*, *37*, 9838–9850.

Moreau, M., Valentin, P., Vidal-Madjar, C., Lin, B. C., & Guiochon, G. (1991). Adsorption isotherm model for multicomponent adsorbate-adsorbate interactions. *Journal of Colloid and Interface Science*, *141*(1), 127–136.

Nathans, D., & Smith, H. O. (1975). Restriction endonucleases in the analysis and restructuring of DNA molecules. *Annual Review of Biochemistry*, *44*, 273–293.

Nguyen, T. H., & Chen, K. L. (2007). Role of divalent cations in plasmid DNA adsorption to natural organic matter-coated silica surface. *Environmental Science and Technology*, *41*(15), 5370–5375.

Nguyen, T. H., & Elimelech, M. (2007). Adsorption of plasmid DNA to a natural organic matter-coated silica surface: Kinetics, conformation, and reversibility. *Langmuir*, *23*(6), 3273–3279.

Nielsen, K. M., Johnsen, P. J., Bensasson, D., & Daffonchio, D. (2007). Release and persistence of extracellular DNA in the environment. *Environmental Biosafety Research*, *6*(1–2), 37–53.

Niemiller, M. L., Porter, M. L., Keany, J., Gilbert, H., Fong, D. W., Culver, D. C., Hobson, C. S., Kendall, K. D., Davis, M. A., & Taylor, S. J. (2017). Evaluation of eDNA for groundwater invertebrate detection and monitoring: A case study with endangered Stygobromus (Amphipoda: Crangonyctidae). *Conservation Genetics Resources*, *10*(2), 247–257.

Nishino, T., & Morikawa, K. (2002). Structure and function of nucleases in DNA repair: Shape, grip and blade of the DNA scissors. *Oncogene*, *21*(58 REV. ISS. 8), 9022–9032.

Oldham, C. E., Farrow, D. E., & Peiffer, S. (2013). A generalized Damköhler number for classifying material processing in hydrological systems. *Hydrology and Earth System Sciences*, *17*(3), 1133–1148.

Overballe-Petersen, S., Harms, K., Orlando, L. A., Mayar, J. V., Rasmussen, S., Dahl, T. W., Rosing, M. T., Poole, A. M., Sicheritz-Ponten, T., Brunak, S., Inselmann, S., de Vries, J., Wackernagel, W., Pybus, O. G., Nielsen, R., Johnsen, P. J., Nielsen, K. M., & Willerslev, E. (2013). Bacterial natural transformation by highly fragmented and damaged DNA. *Proceedings of the National Academy of Sciences of the United States of America*, *110*(49), 19860–19865.

Paget, E., Monrozier, L. J., & Simonet, P. (1992). Adsorption of DNA on clay minerals: Protection against DNaseI and influence on gene transfer. *FEMS Microbiology Letters*, *97*(1–2), 31–39.

Pang, L., Abeysekera, G., Hanning, K., Premaratne, A., Robson, B., Abraham, P., Sutton, R., Hanson, C., Hadfield, J., Heiligenthal, L., Stone, D., McBeth, K., & Billington, C. (2020). Water tracking in surface water, groundwater and soils using free and alginate-chitosan encapsulated synthetic DNA tracers. *Water Research*, *184*, 116192.

Pang, L., Heiligenthal, L., Premaratne, A., Hanning, K. R., Abraham, P., Sutton, R., Hadfield, J., & Billington, C. (2022). Degradation and adsorption of synthetic DNA water tracers in environmental matrices. *Science of the Total Environment*, *844*, 157146.

Pang, L., Robson, B., Farkas, K., McGill, E., Varsani, A., Gillot, L., Li, J., & Abraham, P. (2017). Tracking effluent discharges in undisturbed stony soil and alluvial gravel aquifer using synthetic DNA tracers. *Science of the Total Environment*, *592*, 144–152.

Pang, L., Farkas, K., Bennett, G., Varsani, A., Easingwood, R., Tilley, R., Nowostawska, U., & Lin, S. (2014). Mimicking filtration and transport of rotavirus and adenovirus in sand media using DNA-labeled, protein-coated silica nanoparticles. *Water Research*, *62*, 167–179. https://doi.org/10.1016/j.watres.2014.05.055

Paunescu, D., Puddu, M., Soellner, J. O. B., Stoessel, P. R., & Grass, R. N. (2013). Reversible DNA encapsulation in silica to produce ROS-resistant and heat-resistant synthetic DNA 'fossils'. *Nature Protocols*, *8*(12), 2440–2448.

Pawlowski, J., Apotheloz-Perret-Gentil, L., & Altermatt, F. (2020). Environmental DNA: What's behind the term? Clarifying the terminology and recommendations for its future use in biomonitoring. *Molecular Ecology*, *29*(22), 4258–4264.

Payn, R. A., Gooseff, M. N., Benson, D. A., Cirpka, O. A., Zarnetske, J. P., Bowden, W. B., McNamara, J. P., & Bradford, J. H. (2008). Comparison of instantaneous and constant-rate stream tracer experiments through non-parametric analysis of residence time distributions. *Water Resources Research*, *44*(6), W06404.

Peng, B., Liao, P., & Jiang, Y. (2022). Preferential interactions of surface-bound engineered single stranded DNA with highly aromatic natural organic matter: Mechanistic insights and implications for optimizing practical aquatic applications. *Water Research*, *223*, 119015.

Petosa, A. R., Jaisi, D. P., Quevedo, I. R., Elimelech, M., & Tufenkji, N. (2010). Aggregation and deposition of engineered nanomaterials in aquatic environments: Role of physicochemical interactions. *Environmental Science and Technology*, *44*(17), 6532–6549.

Pietramellara, G., Ascher, J., Borgogni, F., Ceccherini, M. T., Guerri, G., & Nannipieri, P. (2009). Extracellular DNA in soil and sediment: Fate and ecological relevance. *Biology and Fertility of Soils*, *45*(3), 219–235.

Pietramellara, G., Ascher, J., Ceccherini, M. T., Nannipieri, P., & Wenderoth, D. (2007). Adsorption of pure and dirty bacterial DNA on clay minerals and their transformation frequency. *Biology and Fertility of Soils*, *43*(6), 731–739.

Pietramellara, G., Ascher, J., Ceccherini, M. T., & Renella, G. (2002). Soil as a biological system. *Annals of Microbiology*, *52*(2), 119–131.

Pinay, G., Clément, J. C., & Naiman, R. J. (2002). Basic principles and ecological consequences of changing water regimes on nitrogen cycling in fluvial systems. *Environmental Management*, *30*(4), 481–491.

Praetorius, A., Badetti, E., Brunelli, A., Clavier, A., Gallego-Urrea, J. A., Gondikas, A., Hassellöv, M., Hofmann, T., Mackevica, A., Marcomini, A., Peijnenburg, W., Quik, J. T. K., Seijo, M., Stoll, S., Tepe, N., Walch, H., & von der Kammer, F. (2020). Strategies for determining heteroaggregation attachment efficiencies of engineered nanoparticles in aquatic environments. *Environmental Science: Nano*, *7*(2), 351–367.

Praetorius, A., Labille, J., Scheringer, M., Thill, A., Hungerbühler, K., & Bottero, J. Y. (2014). Heteroaggregation of titanium dioxide nanoparticles with model natural colloids under environmentally relevant conditions. *Environmental Science and Technology*, *48*(18), 10690–10698.

Ptak, T., Piepenbrink, M., & Martac, E. (2004). Tracer tests for the investigation of heterogeneous porous media and stochastic modelling of flow and transport–A review of some recent developments. *Journal of Hydrology*, *294*(163), 122–163.

Puddu, M., Paunescu, D., Stark, W. J., & Grass, R. N. (2014). Magnetically recoverable, thermostable, hydrophobic DNA/silica encapsulates and their application as invisible oil tags. *ACS Nano*, *8*(3), 2677–2685.

Purcel, E. A. (1977). Life at low Reynolds number. *American Journal of Physics*, *45*(1), 3–11.

Richter, D., Goeppert, N., & Goldscheider, N. (2022). New insights into particle transport in karst conduits using comparative tracer tests with natural sediments and solutes during low-flow and high-flow conditions. *Hydrological Processes*, *36*(1), e14472.

Rodriguez-Ezpeleta, N., Morissette, O., Bean, C. W., Manu, S., Banerjee, P., Lacoursiere-Roussel, A., Beng, K. C., Alter, S. E., Roger, F., Holman, L. E., Stewart, K. A., Monaghan, M. T., Mauvisseau, Q., Mirimin, L., Wangensteen, O. S., Antognazza, C. M., Helyar, S. J., de Boer, H., Monchamp, M. E., … Deiner, K. (2021). Trade-offs between reducing complex terminology and producing accurate interpretations from environmental DNA: Comment on "Environmental DNA: What's behind the term?" by Pawlowski et al., (2020). *Molecular Ecology*, *30*(19), 4601–4605.

Sabir, I. H., Haldorsen, S., Torgersen, J., & Aleström, P. (1999). DNA tracers with information capacity and high detection sensitivity tested in groundwater studies. *Hydrogeology Journal*, *7*(3), 264–272.

Schijven, J. F., & Šimůnek, J. (2002). Kinetic modeling of virus transport at the field scale. *Journal of Contaminant Hydrology*, *55*(1–2), 113–135.

Schiperski, F., Zirlewagen, J., & Scheytt, T. (2016). Transport and attenuation of particles of different density and surface charge: A karst aquifer field study. *Environmental Science and Technology*, *50*(15), 8028–8035.

Serapinas, S., Gineityte, J., Butkevicius, M., Danilevicius, R., Dagys, M., & Ratautas, D. (2022). Biosensor prototype for rapid detection and quantification of DNase activity. *Biosensors & Bioelectronics*, *213*, 114475.

Sharma, A., Foppen, J. W., Banerjee, A., Sawssen, S., Bachhar, N., Peddis, D., & Bandyopadhyay, S. (2021). Magnetic nanoparticles to unique DNA tracers: Effect of functionalization on physico-chemical properties. *Nanoscale Research Letters*, *16*(1), 24.

Sharma, A. N., Luo, D., & Walter, M. T. (2012). Hydrological tracers using nanobiotechnology: Proof of concept. *Environmental Science and Technology*, *46*(16), 8928–8936.

Simões, E. F. C., Almeida, A. S., Duarte, A. C., & Duarte, R. M. B. O. (2021). Assessing reactive oxygen and nitrogen species in atmospheric and aquatic environments: Analytical challenges and opportunities. *TrAC Trends in Analytical Chemistry*, *135*, 116149.

Siuda, W., Chróst, R. J., & Güde, H. (1998). Distribution and origin of dissolved DNA in lakes of different trophic states. *Aquatic Microbial Ecology*, *15*(1), 89–96.

Smoluchowski, M.v. (1917). Grundriß der Koagulationskinetik kolloider Lösungen. *Kolloid-Zeitschrift*, *21*(3), 98–104.

Suzuki, T., Ohsumi, S., & Makino, K. (1994). Mechanistic studies on depurination and apurinic site chain breakage in oligodeoxyribonucleotides. *Nucleic Acids Research*, *22*(23), 4997–5003.

Taberlet, P., Coissac, E., Hajibabaei, M., & Rieseberg, L. H. (2012). Environmental DNA. *Molecular Ecology*, *21*(8), 1789–1793.

Takeda, K., Takedoi, H., Yamaji, S., Ohta, K., & Sakugawa, H. (2004). Determination of hydroxyl radical Photoproduction rates in natural waters. *Analytical Sciences*, *20*(1), 153–158.

Tang, Y., Foppen, J. W., & Bogaard, T. A. (2021). Transport of silica encapsulated DNA microparticles in controlled instantaneous injection open channel experiments. *Journal of Contaminant Hydrology*, *242*, 103880.

Tang, Y., Zhang, F., Bogaard, T., Chassagne, C., Ali, Z., Bandyopadhyay, S., & Foppen, J. W. (2023). Settling of superparamagnetic silica encapsulated DNA microparticles in river water. *Hydrological Processes*, *37*(1), 1–12.

Tazioli, A., Aquilanti, L., Clementi, F., Marcellini, M., Nanni, T., Palpacelli, S., Roncolini, A., & Vivalda, P. M. (2019). Flow parameters in porous alluvial aquifers evaluated by multiple tracers. *Rendiconti Online Della Società Geologica Italiana*, *47*, 126–132. https://doi.org/10.3301/rol.2019.23

Thakuria, R., Nath, N. K., & Saha, B. K. (2019). The nature and applications of π–π interactions: A perspective. *Crystal Growth & Design*, *19*(2), 523–528.

Trauscht, J., Pazmino, E., & Johnson, W. P. (2015). Prediction of nanoparticle and colloid attachment on unfavourable mineral surfaces using representative discrete heterogeneity. *Langmuir*, *31*(34), 9366–9378.

Tufenkji, N., & Elimelech, M. (2004). Correlation equation for predicting single-collector efficiency in physicochemical filtration in saturated porous media. *Environmental Science and Technology*, *38*(2), 529–536.

Urresti-Estala, B., Vadillo-Pérez, I., Jiménez-Gavilán, P., Soler, A., Sánchez-García, D., & Carrasco-Cantos, F. (2015). Application of stable isotopes (δ34S-SO4, δ18O-SO4, δ15N-NO3, δ18O-NO3) to determine natural background and contamination sources in the Guadalhorce River basin (southern Spain). *Science of the Total Environment*, *506-507*, 46–57.

van den Berg-Stein, S., Hahn, H. J., Thielsch, A., & Schwenk, K. (2022). Diversity and dispersal of aquatic invertebrate species from surface and groundwater: Development and application of microsatellite markers for the detection of hydrological exchange processes. *Water Research*, *210*, 117956.

Wang, C., Liu, G., McNew, C. P., Volkmann, T. H. M., Pangle, L., Troch, P. A., Lyon, S. W., Kim, M., Huo, Z., & Dahlke, H. E. (2022). Simulation of experimental synthetic DNA tracer transport through the vadose zone. *Water Research*, *223*, 119009.

Xu, L., Xu, M., Wang, R., Yin, Y., Lynch, I., & Liu, S. (2020). The crucial role of environmental coronas in determining the biological effects of engineered nanomaterials. *Small*, *16*(36), 2003691.

Xue, J., & Feng, Y. (2018). Determination of adsorption and desorption of DNA molecules on freshwater and marine sediments. *Journal of Applied Microbiology*, *124*(6), 1480–1492.

Yan, C., Cheng, T., & Shang, J. (2019). Effect of bovine serum albumin on stability and transport of kaolinite colloid. *Water Research*, *155*, 204–213.

Yan, J., & Marko, J. F. (2004). Localized single-stranded bubble mechanism for cyclization of short double helix DNA. *Physical Review Letters*, *93*(10), 108108-108101-108108-108104.

Yang, S. P., Bar-Ilan, O., Peterson, R. E., Heideman, W., Hamers, R. J., & Pedersen, J. A. (2013). Influence of humic acid on titanium dioxide nanoparticle toxicity to developing zebrafish. *Environmental Science and Technology*, *47*(9), 4718–4725.

Yang, X., Zhang, Y., Chen, F., & Yang, Y. (2015). Interplay of natural organic matter with flow rate and particle size on colloid transport: Experimentation, visualization, and modeling. *Environmental Science & Technology*, *49*(22), 13385–13393.

Zhai, H., Wang, L., & Putnis, C. V. (2019). Molecular-scale investigations reveal noncovalent bonding underlying the adsorption of environmental DNA on mica. *Environmental Science & Technology*, *53*(19), 11251–11259.

Zhang, Y., Manley, T. S., Li, K., & Home, R. N. (2015). DNA-Encapsulated silica nanoparticle tracers for fracture characterization. *39*, 967–974. 39th Geothermal Resources Council Annual Meeting - Geothermal: Always On, GRC 2015 Reno.

Zhang, X., Li, J., Yao, M. C., Fan, W. Y., Yang, C. W., Yuan, L., & Sheng, G. P. (2020). Unrecognized contributions of dissolved organic matter inducing photodamages to the decay of extracellular DNA in waters. *Environmental Science & Technology*, *54*(3), 1614–1622.

Zhang, Y., Hartung, M. B., Hawkins, A. J., Dekas, A. E., Li, K., & Horne, R. N. (2021). DNA tracer transport through porous media—The effect of DNA length and adsorption. *Water Resources Research*, *57*(2), e2020WR028382.

Zhang, Y., & Huang, T. (2022). DNA-based tracers for the characterization of hydrogeological systems—Recent advances and new Frontiers. *Water*, *14*(21), 3545.

How to cite this article: Foppen, J. W. (2023). Artificial DNA in hydrology. *WIREs Water*, e1681. https://doi.org/10.1002/wat2.1681